



HAL
open science

Effect of Temperature on the Cyclic Behavior of Clay-structure Interface

Soheib Maghsoodi, Olivier Cuisinier, Farimah Masrouri

► **To cite this version:**

Soheib Maghsoodi, Olivier Cuisinier, Farimah Masrouri. Effect of Temperature on the Cyclic Behavior of Clay-structure Interface. *Journal of Geotechnical and Geoenvironmental Engineering*, 2020, 146 (10), 10.1061/(ASCE)GT.1943-5606.0002360 . hal-02888748

HAL Id: hal-02888748

<https://hal.science/hal-02888748>

Submitted on 3 Jul 2020

HAL is a multi-disciplinary open access archive for the deposit and dissemination of scientific research documents, whether they are published or not. The documents may come from teaching and research institutions in France or abroad, or from public or private research centers.

L'archive ouverte pluridisciplinaire **HAL**, est destinée au dépôt et à la diffusion de documents scientifiques de niveau recherche, publiés ou non, émanant des établissements d'enseignement et de recherche français ou étrangers, des laboratoires publics ou privés.

Effect of Temperature on the Cyclic Behavior of Clay-structure

Interface

Soheib Maghsoodi^{1,2*}, Olivier Cuisinier¹, and Farimah Masrouri¹

¹Université de Lorraine, LEMTA (UMR-7563), CNRS, Nancy, France

²École supérieure d'ingénieurs des travaux de la construction de Metz, Metz, France

*Corresponding author: Soheib Maghsoodi, Ph.D. student, Université de Lorraine,

Laboratoire d'énergétique et de Mécanique Théorique et Appliquée,
2 Rue du Doyen Marcel Roubault, 54518, Vandœuvre-les-Nancy Cedex

soheib.maghsoodi@univ-lorraine.fr

¹Olivier Cuisinier, Associate professor, Université de Lorraine

Laboratoire d'énergétique et de Mécanique Théorique et Appliquée,
2 Rue du Doyen Marcel Roubault, 54518, Vandœuvre-les-Nancy Cedex

Olivier.cuisinier@univ-lorraine.fr,

¹Farimah Masrouri, Professor, Université de Lorraine

Laboratoire d'énergétique et de Mécanique Théorique et Appliquée,
2 Rue du Doyen Marcel Roubault, 54518, Vandœuvre-les-Nancy Cedex

Farimah.masrouri@univ-lorraine.fr,

9 **ABSTRACT**

10 The shaft capacity of foundations highly depends on the monotonic and cyclic loads applied
11 to the soil-structure interface. In energy geostructures which exploit the heat of soil using earth-
12 contact elements, the interface is subjected to cyclic thermo-mechanical loads. Monotonic and
13 cyclic constant-volume equivalent-undrained (CVEU) direct shear tests were performed on clay-
14 clay and clay-structure interface at different temperatures (22 and 60 °C). An effective vertical stress
15 of 300 kPa was applied to the samples and the cyclic and average shear stress ratios (τ_{cy}/S_u^{Ds} and
16 τ_a/S_u^{Ds} , respectively) were varied between 0.35 and 0.57. The tested soil was a kaolin clay (PI=24)
17 prepared in a normally consolidated state. The results showed that, the number of cycles to failure
18 for the clay-structure interface test was lower than that for the clay-clay case in the same range of
19 cyclic and average shear stress ratios. In cyclic clay-structure tests, decreasing the cyclic stress
20 ratio, increased the number of cycles to failure; however decreasing the average shear stress ratio
21 decreased the number of cycles to failure. Increasing the temperature, decreased the rate of strain
22 accumulation and the number of cycles to failure increased by 2-3 times. The rate of degradation
23 (degradation parameter, t) decreased by 16% with heating from 22 to 60 °C for the different cyclic
24 stress ratios tested.

25 **Keywords: energy geostructures, soil-structure interface, temperature, cyclic loads, strain**
26 **accumulation**

INTRODUCTION

Incorporation of heat exchangers in conventional geostructures like piles can extract the heat from the soil for heating purposes and inject it to the soil for cooling purposes. The heat exchanger absorber pipes are attached to the reinforcement cage of geostructures (Brandl 2006). In recent years, research has been conducted at full and laboratory scale to investigate the effect of temperature on the geotechnical behavior of these energy geostructures as well as on the surrounding soil (e.g. Laloui et al. 2006; Bourne-Webb et al. 2009; Murphy et al. 2015; Faizal et al. 2018). These energy geostructures can be subjected to cyclic mechanical loads and thermal variations throughout their lifetime. The soil-structure interface, plays a key role in the transmission of the loads to the ground. According to the observations in experimental results, soil-structure interface is a composite of the structural surface and a thin-layer soil nearby which develops a strain localization caused by the transmission of shear force of structure to the soil (Pra-ai and Boulon 2017). Mechanical behavior of interface, which differs from the surrounding soil, depends on the stress state, roughness of the structural surface, density, state of the soil and constant normal stiffness conditions. It is known that cyclic loads evolve the shear resistance of the soil-structure interface and thus the shaft capacity of the structure. Several studies have been performed on the cyclic behavior of sand-structure interface (Potyondy 1961; Desai et al. 1985; Boulon and Foray 1986; Uesugi and Kishida 1986; Poulos and Al-Douri 1992; Jardine et al. 1993; Lehane et al. 1993; Fakharian and Evgin 1997; Mortara et al. 2007; Pra-ai and Boulon 2017), while less is known about the behavior of clay-structure interface (Lemos and Vaughan 2000, Di Donna et al. 2015). In this context, the objective of this study is to investigate the effect of temperature on the cyclic behavior of clay-structure interface. In the following the current knowledge of the influencing parameters on the cyclic behavior of soil and soil-structure interface is discussed.

Saturated clays under cyclic loading in undrained and isothermal conditions, develop accumulation of deformation and generation of excess pore water pressure with increase in number of cycles, which cause shear strength reduction and induce failure (Mortezaie and Vucetic 2013). The shear stress-strain curve of a soil under cyclic loading can be decomposed into average (τ_a) and cyclic

54 shear stress (τ_{cy}) components, while the deformation can be seen as the combination of permanent
55 shear strain (ϵ_p) and cyclic shear strain (ϵ_{cy}) (Fig. 1a). Several parameters, such as the average
56 shear stress, cyclic shear stress, loading frequency (f), strain rate ($\dot{\epsilon}$), number of cycles (N), normal
57 stress (σ_n), temperature (T^o) and initial state of the soil (normally consolidated or overconsolidated)
58 are mentioned as influencing factors on cyclic response of soils (Andersen et al. 1980; Yasuhara
59 et al. 1982; Matasović and Vucetic 1995; Zhou and Gong 2001; Moses et al. 2003; Lackenby et al.
60 2007; Andersen 2009; Li et al. 2011; Wichtmann et al. 2013). Several studies showed that the
61 number of cycles to failure, N_f , decreases with increasing cyclic shear stress (τ_{cy}), but for a given
62 cyclic shear stress (τ_{cy}), a cyclic loading with a lower average shear stress (τ_a) causes failure in
63 fewer cycles than a cyclic loading applied at higher average shear stress (τ_a) (Wichtmann et al.
64 2013). In undrained conditions, volumetric changes are prevented and the effective stresses in the
65 soil decrease with pore pressure buildup (u_p) (Fig. 1b). The excess pore-water pressure generated
66 during cyclic loading depends on the amplitude of the cyclic shear strain or stress, the number
67 of cycles, the frequency of cyclic loading and the overconsolidation ratio (Yasuhara et al. 1982;
68 Ohara and Matsuda 1988). Cyclic stress or strain induced deformation accumulation and excess
69 pore pressure lead to soil degradation and can induce failure (Seed and Chan 1966; Andersen et al.
70 1980; Thian and Lee 2017). Idriss et al. 1976 and Idriss et al. 1978 introduced the degradation
71 index (δ) and the degradation parameter (t), that for the stress-controlled tests can be determined
72 as follows:

$$73 \quad \delta = \frac{G_{SN}}{G_{S1}} = \frac{\tau_c / \epsilon_{cyN}}{\tau_c / \epsilon_{cy1}} = \frac{\epsilon_{cy1}}{\epsilon_{cyN}} \quad (1)$$

$$74 \quad t = -\frac{\log \delta(N)}{\log N} \quad (2)$$

75 where G_{S1} and G_{SN} are the secant moduli at cycles 1 and N , τ_c is the shear stress value, ϵ_{cy1} and
76 ϵ_{cyN} are the cyclic shear strains at cycles 1 and N , respectively. The degradation index can be seen
77 as a mean to evaluate the rate of strain accumulation and the ratio of the cyclic strain at cycles

78 1 and N . Soil with a high δ value will have a low degree of degradation (Zhou and Gong 2001).
79 The average degradation parameter, t , is the slope of the δ vs N line in a log-log scale, which
80 describes the rate of cyclic degradation with N . Studies have shown that the degradation parameter
81 depends on the plasticity index and OCR of the soil (Vucetic and Dobry 1988; Tan and Vucetic
82 1989). The degradation parameter, t , consistently decreases with an increase in the OCR (Soralump
83 and Prasomsri 2015). Soltani and Soroush 2010 showed that there was an increase in the degree
84 of degradation as the number of loading cycles and cyclic shear strain amplitude increased. In
85 cyclic strain-controlled tests carried out on kaolinite in simple shear device, Mortezaie and Vucetic
86 2013 found that in larger cyclic shear strain amplitudes, increase of frequency (f), accelerates the
87 degradation but in higher vertical stresses (σ'_{vc}) the degradation decreases. Frequency is influenced
88 by the strain rate in cyclic simple and direct shear tests and the strain rate can have crucial impacts
89 on the shear strength and volumetric behavior during shearing. Martinez and Stutz 2018 have
90 performed interface monotonic direct shear tests on kaolin clay-steel interface with different strain
91 rates to investigate the interface behavior under drained and undrained conditions. They found by
92 increasing the shearing velocity, the undrained behavior was observed by smaller interface strength
93 and volumetric changes.

94 Very few studies have been carried out on the effect of temperature on cyclic behavior of soils.
95 Cekerevac and Laloui 2010 performed temperature-controlled cyclic triaxial tests on kaolin samples.
96 The samples were consolidated under 600 kPa and heated up to 90 °C in drained conditions and were
97 cyclically sheared under undrained conditions. They found that the initial cycle imposed at either
98 ambient or high temperature produced almost the same axial strain and pore pressure. However
99 later shear cycles of the heated sample induced smaller strain and smaller pore-water pressure per
100 cycle. The number of cycles to failure increased for heated samples due to the densification of clay
101 under drained heating and also the pore pressure of heated samples was slightly less than unheated
102 ones. Xiong et al. 2018 performed cyclic triaxial tests at different temperatures on a saturated soft
103 clay. They showed that the cumulative plastic strain, pore pressure and dynamic damping ratio of
104 saturated clay decreased with increasing temperature, while the dynamic modulus increased with

105 increasing temperature, and the soft clay showed thermal hardening behavior.

106 Regarding the impact of temperature on the soil-structure interface, some experimental studies
107 have been performed (Di Donna et al. 2015; Yavari et al. 2016; Li et al. 2018; Maghsoodi et al.
108 2019b; Yazdani et al. 2019) on direct shear device and concerning the in-situ behavior; Murphy
109 and McCartney 2014 have developed a thermal borehole shear device to study effect of temperature
110 on the in-situ shear behavior of soil-concrete interfaces, but to the knowledge of the authors very
111 few studies have been carried out on the thermal effects on the cyclic behavior of clay-structure
112 interface. Di Donna et al. 2015 performed cyclic constant normal stiffness (CNS) two-way strain
113 controlled tests at different temperatures on illite clay. They revealed that testing clay-concrete
114 samples under CNS conditions at higher temperatures, reduces the volumetric contraction during
115 cyclic shearing and the material becomes denser therefore, more cycles are required to degrade the
116 interface strength.

117 In this context, this study was focused on the one-way cyclic behavior of clay-structure interface
118 under isothermal or non-isothermal conditions. The effects of two parameters on strain accumu-
119 lation, excess pore water pressure and cyclic degradation were more specifically considered. The
120 first one is the average shear stress (τ_a) that represents the allowable shear stress that is mobilized
121 in the structures once the serviceability starts. The second one is the cyclic shear stress (τ_{cy}) that
122 corresponds to the mechanical solicitations that are imposed to the structure during its lifetime once
123 the average shear stress is reached.

124 The following aspects that influence the cyclic behavior of clay-structure interface are addressed:

- 125 • The mechanical monotonic and cyclic behavior differences between clay-clay and clay-structure
126 interface.
- 127 • The effect of average and cyclic shear stress variations (τ_a/S_u^{Ds} and τ_{cy}/S_u^{Ds}) on clay-structure
128 interface cyclic behavior at different temperatures.
- 129 • The effect of temperature on the strain accumulation, equivalent pore water pressure, cyclic loop
130 shape and degradation behavior of the clay-structure interface.

131 THE SHEAR DEVICE, SAMPLE PREPARATION AND THE EXPERIMENTAL PROGRAM

Material properties

The physical and thermal properties of kaolin clay used in this study are presented in Table 1. To perform clay-structure interface direct shear tests, a stainless steel plate (80 x 60 x 10 mm) with the desired roughness was designed and used as the structure to avoid the surface abrasion due to test repetition. The roughness of the steel plate was measured with a laser profilometer. Several profiles parallel to the shear direction were measured. The heights of these four profiles that were obtained with the laser are presented in (Fig. 3a). Fig. 3b shows the height of the one of the profiles in a closer view. The measured average roughness R_a for the profiles was $20 \mu m$, therefore, the plate was considered as a rough surface for clay-structure interface (Maghsoodi et al. 2019a, Maghsoodi et al. 2019c).

The temperature-controlled direct shear device

Fig. 2 shows the configuration of the temperature-controlled direct shear device. The shear box (60 x 60 x 35 mm) was placed inside a container filled with water to reach saturated conditions (Fig. 2). The circulating fluid at the bottom of the shear box container was connected to a thermal regulation system. In such a setup, the temperature of the fully saturated shear box container can be controlled by three thermocouples, one in the lower half of the shear box, another on the upper half of the shear box and the last one in the container. The device can be programmed either in stress or deformation controlled tests (Maghsoodi et al. 2019b). The lower half shear box is displaced horizontally to apply the shear.

Sample preparation

To perform the clay-clay and clay-structure shear tests, a slurry of kaolin clay with a water content of 63%, which was slightly higher than its liquid limit ($LL = 57\%$) was prepared and left for 24 hours for homogenization. Subsequently, the clay was poured into the shear box and special attention was paid to avoid trapping any air. Then, the shear box was placed inside the fully saturated shear box container. Afterwards, the normal stress was applied incrementally during the consolidation phase, each load increment lasted 2 hours and the last step (300 kPa) was left 8 hours to ensure full consolidation. The consolidation phase took 24 hours. Based on the consolidation

159 tests performed on this kaolin clay, the final void ratio after consolidation for $\sigma'_{n0} = 300$ kPa was
160 $e = 0.85$. For tests at 60 °C, a heating rate of 5 °C/hr was applied and left for 4 hours to ensure
161 the fully thermal consolidation of the clay under constant normal stress conditions (300 kPa).

162 **Experimental program**

163 To apply equivalent-undrained conditions in the clay-structure interface tests, the constant-
164 volume equivalent-undrained (CVEU) concept was used in this study. In the extreme case of the
165 constant normal stiffness condition, constant volume case ($K = \infty$ (kPa/mm)), the vertical stress is
166 varied to keep the volume of the sample constant. In the studies using this concept, as conducted
167 by [Vucetic and Lacasse 1984](#); [Dyvik et al. 1987](#) and [Mortezaie and Vucetic 2016](#), during shearing,
168 in drained conditions while the pore pressure was zero, the change in the vertical stress to keep the
169 volume of the sample constant was equivalent to the pore pressure generated in a truly undrained
170 triaxial test. Several studies have confirmed this approach, using direct shear device ([Takada 1993](#);
171 [Hanzawa et al. 2007](#)). [Takada 1993](#) have introduced the direct shear device that is capable to
172 perform constant volume equivalent undrained tests and they have confirmed the capability of the
173 direct shear device to perform CVEU tests. [Hanzawa et al. 2007](#) have performed a comparative
174 study of the NGI Direct Simple Shear Test (DSST) and the Direct Shear Test (DST). Samples
175 from Norwegian Drammen clay and Japanese Ariake clay were subjected to both types of test.
176 They found that the DST test gave generally higher stiffness and strength than the DSST. They
177 explained these differences that can mainly be accounted for by the different shearing mechanisms
178 and shearing rates.

179 The experimental program proposed in this study is based on constant-volume equivalent-
180 undrained (CVEU) concept. As it was shown in Fig. 1, the shear cycles consisted of average
181 and cyclic shear stresses. The objective of this study is to vary these two components of the
182 shear stress in a way that reproduces probable cases of interfaces in energy geostuctures under
183 cyclic loading. Therefore, in order to cover a wide range of stress ratios and also apply diverse
184 cyclic paths that can be subjected to the structure, different ranges of cyclic and stress ratios that
185 are mentioned in literature were chosen ([Wichtmann et al. 2013](#); [Thian and Lee 2017](#); [Zhou and](#)

186 [Gong 2001](#)). The experimental program consisted of monotonic and cyclic CVEU clay-clay and
187 clay-structure interface direct shear tests at different temperatures (Table 2 and Table 3) and it is
188 presented in Fig. 4. The monotonic program consisted of clay-clay and clay-structure interface
189 tests to determine the essential parameters for cyclic experimental program such as S_u^{Ds} (undrained
190 shear strength in direct shear, Fig. 4). Additionally, the monotonic program can be considered as a
191 reference, to better understand the cyclic behavior of clay-clay and clay-structure interface. After
192 the consolidation (or consolidation+heating) phase, for monotonic tests different deformation rates
193 were applied ($\dot{P}_d = 0.01, 0.02\%/min$). Based on [ASTM 1998](#), the relative lateral displacement,
194 is defined as the changes in horizontal displacement, $\Delta W(mm)$ divided by the initial length of the
195 sample ($l_0 = 60$ mm).

196 The cyclic program consisted of two parts. The first part, cyclic clay-clay test was performed
197 to investigate the differences in the cyclic behavior between clay-clay and clay-structure interface.
198 The second part was dedicated to the cyclic clay-structure interface tests at different temperatures.
199 For cyclic tests, the shear stress was increased to the average value (τ_a , path 1-2 in Fig. ??) and
200 then the shear cycles fluctuated in a regular manner between $\tau_a + \tau_{cy}$ and $\tau_a - \tau_{cy}$ with a frequency
201 of 0.005 Hz. The cycles were continued until a relative lateral displacement of 10% was reached.
202 Failure was defined when the relative lateral displacement reached 10%. The volume of the sample
203 was kept constant throughout the tests. Two types of tests were performed, the first one consisted
204 of a constant average shear stress ratio τ_a/S_u^{Ds} (ASR) while varying the cyclic shear stress ratio
205 τ_{cy}/S_u^{Ds} (CSR). The second type was performed with a constant cyclic stress ratio τ_{cy}/S_u^{Ds} but the
206 average stress ratio τ_a/S_u^{Ds} was changed. The objective of the first type was to investigate the effect
207 of cyclic shear stress and the second one was the effect of average shear stress on the cyclic behavior
208 of clay-structure interface. The cyclic stress ratio τ_{cy}/S_u^{Ds} between 0.35 and 0.57 and the average
209 stress ratio τ_a/S_u^{Ds} between 0.38 and 0.47 were chosen.

210 EXPERIMENTAL RESULTS

Monotonic CVEU clay-clay and clay-structure interface tests

To determine the undrained shear strength in direct shear (S_u^{Ds}) test and to investigate the cyclic behavior of clay-clay and clay-structure interface, monotonic clay-clay and clay-structure tests were performed. The comparison of the results obtained during the monotonic tests of the clay-clay and clay-structure constant-volume equivalent-undrained (CVEU) shear tests highlighted some significant differences (Fig. 5). The peak shear stress for the clay-structure tests are around 1-1.5% of relative lateral displacement, while for the clay-clay tests the peak occurs in larger relative lateral displacements (2-3%). Afterwards the strain softening for clay-structure tests occurred at smaller relative lateral displacements (2%) compared to the clay-clay tests which started from 4% and continued until the end of the test. These observations confirmed that the shear occurred in the interface zone.

Fig. 5b shows the variation in the effective normal stress with relative lateral displacement. Due to the normally consolidated state of the soil and to keep the volume of the sample constant, the effective normal stress decreased with shearing for both clay-clay and clay-structure tests. In the clay-clay case the effective normal stress started to decrease from the beginning of the test and after a relative lateral displacement of 6% it remained unchanged. For the clay-structure tests the effective normal stress (σ'_n) up to a relative lateral displacement of 2.5% was completely superimposed on the clay-clay behavior. From 2.5 to 12% σ'_n decreased more for clay-clay compared to clay-structure interface. This can be explained by the thickness of the shear band and different shearing modes at the shearing plane between clay-clay and clay-structure samples. Several studies confirmed that the volumetric response (normal stress/pore water pressure variations in CVEU concept) is strongly influenced by different shearing modes at the interface zone (mode I, II and III) (Littleton 1976, Lupini et al. 2009, Tsubakihara et al. 1993). Mode I is a complete shear in the soil mass, mode II is the sliding at the interface and mode III is a combination between mode I and II. Tsubakihara et al. 1993 performed clay-clay and clay-steel interface tests with different roughness. They mentioned for $R_{max} = 20\mu m$ (the same roughness of the steel plate used in this study), the shearing mode can be considered as type III. In mode III, a combination of mode I and II, partially sliding at the

238 interface occurs. In some parts of shearing plane, clogging of clay particles between asperities takes
239 place and on the other parts full sliding is dominant. The same trends as Fig. 5b can be observed
240 for the equivalent pore pressure (Fig. 5c). From 2.5 to 12% of relative lateral displacement, the
241 equivalent pore pressure that was generated for clay-clay was higher than the clay-structure tests.
242 The thickness of clay-clay shear band is greater than clay-structure samples and furthermore, the
243 shearing mode for clay-structure interface tests up to 2.5% of P_d is mode I while from 2 to 2-12%
244 is mode II which can explain the observed behavior. For the Mohr-coulomb plane, Fig. 5d shows
245 the reduction of effective normal stress with increasing the shear stress for both clay-clay and
246 clay-structure interface CVEU tests.

247 **Cyclic behavior at different temperatures**

248 In this section, first, the typical results that can be obtained in one-way CVEU cyclic interface
249 tests are discussed. Then, a comparison between clay-clay and clay-structure cyclic behavior is
250 presented. Finally, the effect of cyclic and average stress ratio variations under non-isothermal
251 conditions on shear strength is discussed in detail.

252 *Typical cyclic results*

253 Fig. 6 shows the typical results of one of the one-way cyclic clay-structure interface tests that
254 was performed ($\tau_a/S_u^{Ds} = 0.41$, $\tau_{cy}/S_u^{Ds} = 0.54$). The shear stress varied between two values of
255 $\tau_a + \tau_{cyc} = 60$ kPa and $\tau_a - \tau_{cyc} = -8$ kPa (Fig. 6a). Cycle numbers 1 and 45 are shown in the figure
256 to better illustrate the permanent deformation accumulation during the test. The relative lateral
257 displacement (δ) raised with increasing number of cycles until a certain value that corresponding
258 to the failure (Fig. 6b). It appears that the first cycle caused a permanent strain of 0.5% and started
259 to increase progressively with the number of cycles toward the failure point (Fig. 6c). The rate
260 of strain accumulation with the number of cycles increased progressively until failure. Finally the
261 failure occurred at around 1.28%. To keep the volume of the clay sample constant during the cyclic
262 shearing phase, the effective normal stress was not constant during the test (Fig. 6d). Due to the
263 normally consolidated state of the clay in this study, the general trend of effective normal stress was
264 decreasing. [Mortezaie and Vucetic 2013](#) found the same decreasing trend of the effective normal

265 stress by cyclic testing of kaolinite in simple shear device. For each cycle, the effective normal
 266 stress during shear load on (from -8 to 60 kPa) increased and during shear load off (from 60 to -8
 267 kPa) decreased. The increase in the equivalent pore pressure due to the first cycle was almost 127
 268 kPa, which is 40% of the initial effective normal stress ($\sigma'_{n0} = 300$ kPa) that was applied (Fig. 6e).
 269 After the first cycle, the equivalent pore pressure (u^*) increased with an almost constant slope.

270 In the degradation index method proposed by [Idriss et al. 1978](#), the degradation index is
 271 calculated as the ratio between the strain of cycle 1 and N (Eq. 1). In this study, this concept was
 272 slightly modified in the context to take into account the fact that the relative lateral displacement of
 273 the first cycles did not start from the same point compared to the works using this method ([Idriss](#)
 274 [et al. 1978](#); [Zhou and Gong 2001](#)), as follows:

$$275 \quad \delta^* = \frac{P_{d(cy1)} + (1 - P_{d(cy1)})}{P_{d(cyN)} + (1 - P_{d(cy1)})} = \frac{1}{P_{d(cyN)} + (1 - P_{d(cy1)})} \quad (3)$$

276 where $P_{d(cy1)}$ and $P_{d(cyN)}$ are the cyclic relative lateral displacement at cycles 1 and N. A
 277 constant value $(1 - P_{d(cy1)})$ is added to both cyclic relative lateral displacements to shift the $P_{d(cy1)}$
 278 so that it starts from 1. Fig. 6f shows the degradation index vs. the number of cycles. The slope
 279 of this curve in a log-log curve is the t parameter. Finally Fig. 6g shows the Mohr-Coulomb plane
 280 of the cyclic test. The above-mentioned types of results are used in the next sections to present the
 281 cyclic behavior of clay-clay and clay-structure interface.

282 *Cyclic behavior of clay-clay vs. clay-structure interface*

283 To investigate the cyclic behavior difference of clay-clay and clay-structure interface, CVEU
 284 cyclic clay-clay and clay-structure interface tests were performed. Both tests were performed with
 285 the same average and cyclic stress ratios ($\tau_a/S_u^{Ds} = 0.41$ and $\tau_{cy}/S_u^{Ds} = 0.47$) (Fig. 7). For the
 286 same average stress ratio (ASR) and cyclic stress ratio (CSR), the number of cycles to failure for the
 287 clay-structure was 185 while for the clay-clay case 370 cycles were necessary to reach failure (Fig.
 288 7a). The accumulated relative lateral displacement (P_{da}) for both cases started from the same point
 289 (0.12%) and increased progressively with number of cycles (Fig. 7b). The strain accumulation for

290 both tests followed the same trend but the P_d corresponding to the failure for clay-structure (1.5%)
291 was less than clay-clay case (3.4%). It can be noticed that, lower excess pore pressure was generated
292 for clay-structure interface test at the end of cycling (Fig. 7c). Similar to the accumulated relative
293 lateral displacement, the pore pressure u^* trend for both cases is consistent. As it was observed in the
294 monotonic part, the equivalent pore pressure (u^*) of clay-clay and clay-structure were superimposed
295 below 2% of P_d (Fig. 5c). Due to the fact the accumulated relative lateral displacement (P_{da}) of
296 cyclic clay-structure interface is less than 2%, the identical curves for u^* was observed. For the
297 degradation index the same scenario was repeated. Both tests followed the same trend, but due
298 to the higher number of cycles to failure for the clay-clay test, the degradation index decreased
299 more for clay-clay test than for clay-structure interface test. The main difference between the cyclic
300 behavior of clay-structure interface and that of clay-clay is the number of cycles to failure, which
301 is lower for the interface case.

302 *Effect of cyclic stress ratio (CSR) variations at different temperatures*

303 After the consolidation, a heating phase with a rate of $5\text{ }^\circ\text{C/hr}$, was applied to the clay-structure
304 interface. The thermal consolidation curve of the clay-structure interface is shown in Fig. 8a.
305 Heating from 22 to $60\text{ }^\circ\text{C}$ caused 0.15 mm of settlement. After reaching the desired temperature
306 ($60\text{ }^\circ\text{C}$), the slope of the thermal consolidation decreased (Fig. 8a). The thermal vertical strain
307 with heating from 22 to 60 was 0.88% (Fig. 8b).

308 For the effect of cyclic stress ratio (CSR) variations at different temperatures, two series of
309 tests with an average shear stress of $\tau_a/S_u^{Ds} = 0.41$ (Fig. 9) and 0.47 (Fig. 10) were performed.
310 For $\tau_a/S_u^{Ds} = 0.41$, the cyclic stress ratio (CSR) varied from 0.35 to 0.57 at different temperatures
311 (22 and $60\text{ }^\circ\text{C}$). Reduction of CSR from 0.57 to 0.35, increased the number of cycles to failure
312 from 39 to 4200 cycles (Fig. 9a). The number of cycles to failure upon cycling at elevated
313 temperatures for all of the different CSR values increased by 2.5-4 times. The accumulated relative
314 lateral displacement (P_{da}) evolution versus the number of cycles is depicted in Fig. 9b. The CSR
315 reduction from 0.57 to 0.35 decreased the relative lateral displacement of the first cycle from 0.48 to
316 0.12%. Heating reduced the ($P_{da(cy1)}$) for $\tau_{cy}/S_u^{Ds} = 0.57$ from 0.42 to 0.13% which is a reduction

317 of 69%. The equivalent pore pressure u^* , of the first cycle was larger when CSR was higher (Fig.
318 9c). Heated samples have lower equivalent pore pressure u^* , than unheated ones. Higher CSR
319 values, raised the degradation index rate (Fig. 9d). For CSR value of 0.35 the degradation index of
320 0.6 was obtained in around 1000 cycles, while for a CSR value of 0.47, the same degradation index
321 could be obtained with only 100 cycles. Considering the effect of temperature, as in the previous
322 observations the degradation index decreased for heated samples and they showed less tendency to
323 degrade compared to unheated samples. The degradation index of 0.6 for the test with CSR of 0.53
324 at 22 °C was obtained in 35 cycles while for the heated sample, it was obtained in 100 cycles.

325 The second series of tests was performed with an average shear stress of $\tau_a/S_u^{Ds} = 0.47$ (Fig. 10)
326 and two different CSR_s of 0.47 and 0.35. The tests with lower CSR values (0.35), were stopped after
327 almost 2000 cycles. The test with $\tau_{cy}/S_u^{Ds} = 0.47$ was performed twice to verify the repeatability of
328 the tests (Fig. 10a). The accumulated relative lateral displacement of the first cycles ($P_{da(cy1)}$) for
329 the CSR values of 0.47 and 0.35 were 0.25 and 0.13% respectively (Fig. 10b). The heated samples
330 showed a lower ($P_{da(cy1)}$) and the rate of strain accumulation was less than that of the unheated
331 samples (Fig. 10b). For the CSR of 0.47 the pore pressure u^* , for cycle 1 was 65-88 kPa, while
332 for CSR=0.35 it was 37 kPa (Fig. 10c). Fig. 10d shows the degradation index with the number
333 of cycles. For heated samples with a CSR of 0.47, in 100 cycles, the degradation index was 0.68,
334 while at 22 °C it was 0.6-0.65.

335 *Effect of average stress ratio (ASR) variations at different temperatures*

336 For the effect of average stress variations τ_a/S_u^{Ds} (ASR), two series of tests with CSR values of
337 0.54 and 0.47 were performed. Fig. 11 shows the results of the test with a CSR of 0.54. The number
338 of cycles to failure reduced from 65 to 46 with decreasing the average shear stress ratio from 0.44
339 to 0.41 (Fig. 11a). Increased number of cycles to failure by 2-2.5 times was the consequence of
340 the heating from 22 to 60 °C. Fig. 11b illustrates the accumulated relative lateral displacement
341 (P_{da}) as a function of number of cycles. For both ASR values of 0.44 and 0.41 at 22 °C, the (P_{da})
342 corresponding to the first cycle started from almost 0.45%. However, for heated samples these
343 values decreased to 0.13%. Fig. 11c shows the value of u^* with the number of cycles. The test with

344 higher ASR generated lower u^* values at 22 °C. For heated samples the generated u^* was less than
345 unheated samples. Taking into account the results of the test with ASR of 0.41, the heated sample
346 had a u^* of 100 kPa at 10 cycles while for unheated sample at the same cycle the u^* was around
347 150 kPa. The degradation evolution during the cycles was presented in Fig. 11d. The degradation
348 index of 0.5 was in 65 cycles for the ASR of 0.41 while for an ASR of 0.44, it was obtained in
349 around 111 cycles. Heating caused a lower degradation index in heated samples compared with that
350 in unheated samples. For the unheated sample with an ASR of 0.41 at 10 cycles, the degradation
351 index was 0.76, while for the heated sample, it was 0.82.

352 Fig. 12 shows the results of the second series of tests with a CSR of 0.47. The average shear
353 stress varies between 0.38 and 0.47. The results clearly indicated that, by reducing the ASR from
354 0.47 to 0.38, the number of cycles to failure decreased from 246 to 57 at 22°C. The heating tended
355 to increase the number of cycles to failure. For an ASR of 0.41 the number of cycles to failure was
356 increased from 185 to 645 cycles for a temperature increase from 22 to 60 °C. For ASR values of
357 0.47, 0.41 and 0.38, the $P_{da(cy1)}$ started from almost 0.25% (Fig. 12b). However for heated samples
358 these values decreased to 0.12%. Fig. 12c shows u^* with number of cycles. For ASR of 0.47 at
359 10 cycles the unheated sample u^* was 114 kPa while for heated sample was around 95 kPa. For
360 heated samples the u^* trend was lower than unheated samples. The degradation index of 0.5 was
361 obtained in 45 cycles for an ASR of 0.38, while for an ASR of 0.41, it was obtained in around 150
362 cycles (Fig. 12d). The degradation of the heated samples was less than that of the unheated ones.
363 For the unheated sample with an ASR of 0.38 at 10 cycles, the degradation index was 0.77, while
364 for the heated sample, it was 0.88.

365 DISCUSSION

366 The recorded results are discussed in this section to clarify (i) the effect of mechanical monotonic
367 and cyclic loads on clay-clay and clay-structure interface, (ii) the effect of cyclic and average stress
368 variations at different temperatures and (iii) the thermal effects on strain accumulation, equivalent
369 pore pressure generation and degradation of clay-structure interface.

370 Fig. 13 presents the monotonic and cyclic constant-volume equivalent-undrained (CVEU) test

371 comparison of the clay-clay and the clay-structure interface. The strain softening in the monotonic
372 test for clay-clay starts around 2.5% while for the clay-structure interface test, it is in lower relative
373 lateral displacements (0.8%). The cyclic solicitations cannot go beyond the monotonic shear stress-
374 strain curve. In other words, when the strain softening started, the capacity for further cycles
375 decreased and due to the fact that the monotonic shear stress is the allowable mobilized shear stress,
376 the cyclic loads cannot exceed the yield limit. The last cycles close to the failure for clay-clay case
377 is around 3-3.5% while for clay-structure test it is about 1.3-1.5%. Therefore, the virgin monotonic
378 curve influences the cyclic behavior of both tests and the reason for lower number of cycles at failure
379 for the clay-structure tests compared with that of the clay-clay test may be due to the difference
380 between the strain softening in the two cases. Andersen 2009 performed post-cycle shear tests after
381 some certain cycles on a clay sample (clay-clay) in simple shear device, to investigate the effect of
382 cyclic loads on static shear strength. The results showed that the post-cyclic shear strength rapidly
383 converged with the virgin monotonic stress-strain curve. The post-cyclic static shear strength of
384 the clay was governed by the virgin monotonic stress-strain curve and the permanent shear strain
385 that was developed during cyclic loading which is in consistent with the observations in this study.

386 To draw conclusions about the observed cyclic behavior difference between clay-clay and clay-
387 structure interface tests, precautions should be taken in practical design calculations for the interface
388 behavior of geostuctures subjected to mechanical cyclic loads.

389 Fig. 14 shows the difference between cyclic loops (N=1, 10 and 100) of the clay-clay and
390 the clay-structure interface tests. The relative lateral displacement at the beginning of the cycles
391 is subtracted, and they all started from zero. The slope of the clay-structure loading-unloading
392 hysteresis is higher than that of the clay-clay case for the cycles mentioned. For N=1 the area
393 encompassed by the clay-structure is smaller than clay-clay case which implies that the energy
394 dissipated in clay-clay case is more than clay-structure interface. Despite the steeper loading-
395 unloading hysteresis loops for clay-structure interface compared to that of the clay-clay, the number
396 of cycles to failure for the clay-structure case is lower than that for the clay-clay case, which confirms
397 the pronounced difference of both cases in terms of shearing plane and strain softening.

398 Fig. 15 shows the cyclic loops for an ASR of 0.41 and CSR_s of 0.57, 0.47 and 0.35 at
399 different temperatures. The cyclic loops of $N=1$ and 10 for a CSR of 0.57 are compared with their
400 counterparts at different temperatures in Fig. 15a and Fig. 15b. The cyclic hysteresis at higher
401 temperatures for $N=1$ and 10 at 60°C are steeper compared to those of the unheated samples which
402 may be due to the denser state of the heated samples. It is also observed that the areas encompassed
403 by the hysteresis loop in heated samples are smaller than those in unheated samples in clay-structure
404 interface tests, implying that less energy is dissipated in heated samples. [Cekerevac and Laloui](#)
405 [2010](#) by performing temperature-controlled undrained cyclic triaxial tests on kaolin have reported
406 that, the cyclic hysteresis loops at higher temperatures are more regular and straighter, with steeper
407 loading-unloading curves compared with those of the heated samples which, is consistent with
408 responses observed in this study. The effect of temperature on hysteresis loops has been reported
409 by [Xiong et al. 2018](#) for saturated soft clay in dynamic triaxial cyclic tests. They observed that,
410 with increasing temperature from 25 to 65°C , the accumulative plastic strain under 10000 cycles
411 decreased from 0.5% to 0.15% ($p' = 50$, $q_{cyc} = 10$ kPa). They compared hysteresis loops of certain
412 cycles, at 25 , 45 and 65°C and reported that, the shear strain of each cycle at 65°C is less than
413 those at 45 and 25°C , which is consistent with the results observed in this study. The reason for the
414 densification of the soil may be the thermoplastic strain generated during the heating process which
415 causes the soil to be thermally overconsolidated. For a CSR of 0.47, the effect of temperature
416 on cyclic loops is less pronounced (Figs. 15c, 15d, 15e). For a CSR of 0.35, there is almost
417 no noticeable difference among $N=10$, 100 and 1000 hysteresis loops at different temperatures
418 compared to those at other CSR values (Figs. 15f, 15g and 15h). The reduction in the CSR value
419 ceases the effect of temperature on cyclic hysteresis loops and the difference between the heated
420 and unheated loops becomes relatively insignificant. This may be due to the fact that, in lower CSR
421 values the cyclic loads are in plastic shakedown but at higher CSR values, the cyclic loads reach the
422 ratcheting response; therefore, the effect of temperature is more pronounced. Based on the three
423 different CSR values compared in Fig. 15, it can be observed that at a CSR less than 0.47 (τ_{cy}/S_u^{Ds}),
424 the effect of temperature on cyclic characteristics of clay-structure interface is negligible. [Mortezaie](#)

425 and Vucetic 2016 by conducting cyclic CVEU simple shear tests on kaolinite have observed that
426 beyond a threshold of cyclic shear strain of $\gamma_{td} = 0.012$ and 0.014% , the degradation rate and pore
427 pressure generation is not evolved with further cycling.

428 The values of the degradation parameter t in Fig. 16 are the slopes of the lines fitted through
429 the logarithm of number of cycles versus logarithm of degradation index data points for cyclic
430 tests. At 22°C with increasing CSR from 0.35 to 0.57, the degradation parameter increases from
431 0.064 to 0.115 but for tests at 60°C the degradation parameter increases from 0.049 to 0.097 for
432 the same range of CSR. The degradation parameters for heated samples are lower than the tests at
433 22°C which can be due to the denser state of the samples that reduces the rate of degradation. The
434 degradation rate for the CSR range between 0.35 to 0.57 decreases about 16% for a temperature
435 increase from 20 to 60°C . On the basis of CVEU simple shear tests on kaolinite (clay-clay type),
436 Mortezaie and Vucetic 2013 have reported that, in the cyclic strain range of $0.1-0.5\%$, with an
437 vertical stress increase from 220 to 680 kPa, degradation parameter reduces by $20-38\%$, which
438 can be comparable to the decrease have been obtained by heating in this study. The thermal
439 overconsolidation phenomena, play the same role as mechanical loading.

440 Fig. 17a shows the variation in the number of cycles to reach different values of relative
441 lateral displacements ($P_d = 0.5, 0.7, 1, 10\%$) with CSR (τ_{cy}/S_u^{Ds}) variations at 22 and 60°C . With
442 decreasing the CSR_s from 0.57 to 0.35 the number of cycles to reach 0.5% of relative lateral
443 displacement increases from 3 to 125 cycles at 22°C . However for the heated samples to reach the
444 same P_d , with the same reduction in the CSR the number of cycles increases from 35 to 452. With
445 decreasing CSR values, the effect of temperature becomes less noticeable. For the CSR of 0.57 at
446 60° to reach 0.5% of P_d , the number of cycles is increased by 4-7 times compared to that at 22°
447 while with decreasing the CSR to 0.35 this ratio becomes 2-4 times. Fig. 17b shows the variation
448 of number of cycles to reach different values of normalized pore pressure ($u^*/\sigma'_{ni} = 0.5, 0.6$) with
449 CSR variations. The number of cycles to reach $u^*/\sigma'_{ni} = 0.5$ is increasing from 5 to 1500 cycles
450 with decreasing the CSR from 0.57 to 0.35 at 22°C . To reach the same normalized pore pressure
451 (0.5) for heated samples the number of cycles increases by 4-6 times.

CONCLUSIONS

This study presents an investigation of the effect of cyclic parameter variations on clay-structure interface behavior at different temperatures (22 and 60 °C). Constant-volume equivalent-undrained (CVEU) monotonic and cyclic clay-clay and clay-structure tests were performed. The strain accumulation, equivalent excess pore pressure, degradation index and stress–strain hysteresis loops are presented and discussed. The following conclusions are obtained:

- In monotonic CVEU tests, the shear behavior of the clay-structure is different from the clay-clay one. The peak, strain softening and effective stress reduction differences confirm that the shear occurs in the interface zone.

The virgin monotonic behavior of the clay-clay and clay-structure interface, shows the limit which the cyclic loads can not go beyond.

- The results clearly show the difference between cyclic behavior of the clay-clay and clay-structure interface tests. The number of cycles to failure for clay-structure test is lower than that for the clay-clay one due to the difference in their strain softening mode.

- In cyclic behavior of interface, decreasing the cyclic stress ratio (CSR) increases the number of cycles to failure and decreases the equivalent pore pressure and degradation index.

- The temperature increase from 22 to 60 °C, substantially increases the number of cycles to failure. For almost all of the cyclic clay-structure interface tests, the relative lateral displacement and equivalent pore pressure corresponding to the first cycle decrease after heating. Drained heating of the normally consolidated kaolin, causes thermal overconsolidation and makes the sample denser, which may be one of the reasons for the increase in the number of cycles to failure. The denser state of the heated samples compared to the unheated samples reduces the rate of degradation.

- Reducing the average shear stress, decreases the number of cycles to failure. The samples are subjected to higher negative shear stresses and therefore, the resistance against cycles are reduced.

- Normally consolidated kaolin clay with the characteristics in this study subjected to cyclic stresses mentioned in this study by heating from 22 to 60 °C, shows higher number of cycles to failure.

Further investigations should be carried out to investigate the effect of monotonic and cyclic

479 temperature variations on the one-way and two-way cyclic behavior of normally consolidated and
480 overconsolidated clay-clay and clay-structure interface.

481 **DATA AVAILABILITY**

482 All data, models, and code generated or used during the study appear in the submitted article.

483 **ACKNOWLEDGMENT**

484 The authors would like to acknowledge Prof. Marc Boulon, Mr. Nicolas Utter (Solétanche
485 Bachy) and Dr. Umur Salih Okyay for fruitful discussions during the meetings.

486 **LIST OF SYMBOLS**

- 487 • ϵ_{cy} Cyclic shear strain
- 488 • ϵ_p Permanent shear strain
- 489 • P_d (%) Relative lateral displacement
- 490 • P_{da} (%) Accumulated relative lateral displacement
- 491 • $P_{da(cy1)}$ (%) Accumulated relative lateral displacement corresponding to the first cycle
- 492 • S_u Undrained shear strength
- 493 • S_u^{DS} Undrained shear strength of direct shear
- 494 • τ (kPa) Shear stress
- 495 • τ_a (kPa) Average shear stress
- 496 • τ_{cy} (kPa) Cyclic shear stress
- 497 • σ'_n (kPa) Effective normal stress
- 498 • $\sigma'_{n,i}$ (kPa) Initial effective normal stress
- 499 • τ_{cy}/S_u^{DS} (-) Cyclic stress ratio (CSR)
- 500 • τ_a/S_u^{DS} (-) Average stress ratio (ASR)
- 501 • ϵ (%) Shear strain
- 502 • u^* (kPa) Equivalent pore-pressure
- 503 • R_n (-) Normalized surface roughness
- 504 • p' (kPa) Confining pressure
- 505 • q_{cyc} (kPa) Cyclic deviatoric stress
- 506 • ρ_s (g/cm³) Grain density of soil particles
- 507 • LL (%) Liquid limit
- 508 • PL (%) Plastic limit
- 509 • PI (%) Plasticity index
- 510 • λ (W/mK) Thermal conductivity
- 511 • C (J/m³K) Heat capacity
- 512 • k (m/s) Hydraulic conductivity

REFERENCES

- Andersen, K. H. (2009). "Bearing capacity under cyclic loading—offshore, along the coast, and on land. the 21st bjerrum lecture presented in oslo, 23 november 2007." *Canadian Geotechnical Journal*, 46(5), 513–535.
- Andersen, K. H., Rosenbrand, W. F., Brown, S. F., and Pool, J. H. (1980). "Cyclic and static laboratory tests on drammen clay." *Journal of the Soil Mechanics and Foundations Division*, 106(5), 499–529.
- ASTM (1998). "Standard test method for direct shear test of soils under consolidated drained conditions." *ASTM standard D3080-98*, West Conshohocken, USA.
- Boulon, M. and Foray, P. (1986). "Physical and numerical simulation of lateral shaft friction along offshore piles in sand." *Proceedings of the 3rd International Conference on Numerical methods in Offshore piling, Nantes, France*, 127–147.
- Bourne-Webb, P., Amatya, B., Soga, K., Amis, T., Davidson, C., and Payne, P. (2009). "Energy pile test at lambeth college, london: geotechnical and thermodynamic aspects of pile response to heat cycles." *Géotechnique*, 59(3), 237–248.
- Brandl, H. (2006). "Energy foundations and other thermo-active ground structures." *Géotechnique*, 56(2), 81–122.
- Cekerevac, C. and Laloui, L. (2010). "Experimental analysis of the cyclic behaviour of kaolin at high temperature." *Géotechnique*, 60(8), 651.
- Desai, C., Drumm, E., and Zaman, M. (1985). "Cyclic testing and modeling of interfaces." *Journal of Geotechnical Engineering*, 111(6), 793–815.
- Di Donna, A., Ferrari, A., and Laloui, L. (2015). "Experimental investigations of the soil–concrete interface: physical mechanisms, cyclic mobilization, and behaviour at different temperatures." *Canadian Geotechnical Journal*, 53(4), 659–672.
- Dyvik, R., Berre, T., Lacasse, S., and Raadim, B. (1987). "Comparison of truly undrained and constant volume direct simple shear tests." *Geotechnique*, 37(1), 3–10.
- Faizal, M., Bouazza, A., Haberfield, C., and McCartney, J. S. (2018). "Axial and radial thermal

541 responses of a field-scale energy pile under monotonic and cyclic temperature changes.” *Journal*
542 *of Geotechnical and Geoenvironmental Engineering*, 144(10), 04018072.

543 Fakharian, K. and Evgin, E. (1997). “Cyclic simple-shear behavior of sand-steel interfaces under
544 constant normal stiffness condition.” *Journal of Geotechnical and Geoenvironmental Engineer-*
545 *ing*, 123(12), 1096–1105.

546 Hanzawa, H., Nutt, N., Lunne, T., Tang, Y., and Long, M. (2007). “A comparative study between the
547 ngi direct simple shear apparatus and the mikasa direct shear apparatus.” *Soils and foundations*,
548 47(1), 47–58.

549 Idriss, I., Dobry, R., Doyle, E., Singh, R., et al. (1976). “Behavior of soft clays under earthquake
550 loading conditions.” *Offshore Technology Conference, Dallas*, Vol. 3.

551 Idriss, I. M., Dobry, R., and Sing, R. (1978). “Nonlinear behavior of soft clays during cyclic
552 loading.” *Journal of geotechnical and geoenvironmental engineering*, 104(ASCE 14265).

553 Jardine, R., Lehane, B., and Everton, S. (1993). “Friction coefficients for piles in sands and silts.”
554 *Offshore site investigation and foundation behaviour*, Springer, 661–677.

555 Lackenby, J., Indraratna, B., McDowell, G., and Christie, D. (2007). “Effect of confining pressure
556 on ballast degradation and deformation under cyclic triaxial loading.” *Géotechnique*, 57(6),
557 527–536.

558 Laloui, L., Nuth, M., and Vulliet, L. (2006). “Experimental and numerical investigations of the
559 behaviour of a heat exchanger pile.” *International Journal for Numerical and Analytical Methods*
560 *in Geomechanics*, 30(8), 763–781.

561 Lehane, B., Jardine, R., Bond, A. J., and Frank, R. (1993). “Mechanisms of shaft friction in sand
562 from instrumented pile tests.” *Journal of Geotechnical Engineering*, 119(1), 19–35.

563 Lemos, L. and Vaughan, P. (2000). “Clay–interface shear resistance.” *Géotechnique*, 50(1), 55–64.

564 Li, C., Kong, G., Liu, H., and Abuel-Naga, H. (2018). “Effect of temperature on behaviour of red
565 clay–structure interface.” *Canadian Geotechnical Journal*, 56(1), 126–134.

566 Li, L.-L., Dan, H.-B., and Wang, L.-Z. (2011). “Undrained behavior of natural marine clay under
567 cyclic loading.” *Ocean Engineering*, 38(16), 1792–1805.

- 568 Littleton, I. (1976). “An experimental study of the adhesion between clay and steel.” *Journal of*
569 *terramechanics*, 13(3), 141–152.
- 570 Lupinl, J., Skinner, A., and Vaughan, P. (2009). “The drained residual strength of cohesive soils.”
571 *Selected papers on geotechnical engineering by PR Vaughan*, Thomas Telford Publishing, 88–
572 120.
- 573 Maghsoodi, S., Cuisinier, O., and Masrouri, F. (2019a). “Comportement thermo-mécanique de
574 l’interface sable-structure.” *17th European Conference on Soil Mechanics and Geotechnical*
575 *Engineering*, <<https://doi.org/10.32075/17ECSMGE-2019-0274>>.
- 576 Maghsoodi, S., Cuisinier, O., and Masrouri, F. (2019b). “Thermal effects on the
577 mechanical behaviour of the soil-structure interface.” *Canadian Geotechnical Journal*,
578 (<https://doi.org/10.1139/cgj-2018-0583>).
- 579 Maghsoodi, S., Cuisinier, O., and Masrouri, F. (2019c). “Thermo-mechanical behaviour of clay-
580 structure interface.” *E3S Web of Conferences*, Vol. 92, EDP Sciences, 10002.
- 581 Martinez, A. and Stutz, H. H. (2018). “Rate effects on the interface shear behaviour of normally
582 and over-consolidated clay.” *Géotechnique*.
- 583 Matasović, N. and Vucetic, M. (1995). “Generalized cyclic-degradation-pore-pressure generation
584 model for clays.” *Journal of geotechnical engineering*, 121(1), 33–42.
- 585 Mortara, G., Mangiola, A., and Ghionna, V. N. (2007). “Cyclic shear stress degradation and post-
586 cyclic behaviour from sand–steel interface direct shear tests.” *Canadian Geotechnical Journal*,
587 44(7), 739–752.
- 588 Mortezaie, A. and Vucetic, M. (2016). “Threshold shear strains for cyclic degradation and cyclic
589 pore water pressure generation in two clays.” *Journal of Geotechnical and Geoenvironmental*
590 *Engineering*, 142(5), 04016007.
- 591 Mortezaie, A. R. and Vucetic, M. (2013). “Effect of frequency and vertical stress on cyclic degra-
592 dation and pore water pressure in clay in the ngi simple shear device.” *Journal of Geotechnical*
593 *and Geoenvironmental Engineering*, 139(10), 1727–1737.
- 594 Moses, G., Rao, S., and Rao, P. (2003). “Undrained strength behaviour of a cemented marine clay

under monotonic and cyclic loading.” *Ocean engineering*, 30(14), 1765–1789.

Murphy, K. D. and McCartney, J. S. (2014). “Thermal borehole shear device.” *Geotechnical Testing Journal*, 37(6), 1040–1055.

Murphy, K. D., McCartney, J. S., and Henry, K. S. (2015). “Evaluation of thermo-mechanical and thermal behavior of full-scale energy foundations.” *Acta Geotechnica*, 10(2), 179–195.

Ohara, S. and Matsuda, H. (1988). “Study on the settlement of saturated clay layer induced by cyclic shear.” *Soils and Foundations*, 28(3), 103–113.

Potyondy, J. G. (1961). “Skin friction between various soils and construction materials.” *Geotechnique*, 11(4), 339–353.

Poulos, H. and Al-Douri, R. (1992). “Influence of soil density on pile skin friction in calcareous sediments.” *Proc., 6th ANZ Conf. on Geomech*, 375–380.

Pra-ai, S. and Boulon, M. (2017). “Soil–structure cyclic direct shear tests: a new interpretation of the direct shear experiment and its application to a series of cyclic tests.” *Acta Geotechnica*, 12(1), 107–127.

Seed, H. B. and Chan, C. K. (1966). “Clay strength under earthquake loading conditions.” *Journal of Soil Mechanics & Foundations Div*, 92(ASCE# 4723 Proceeding).

Soltani, J. H. and Soroush, A. (2010). “Cyclic behavior of mixed clayey soils.” *International Journal of Civil Engineering*, 8(2), 99–106.

Soralump, S. and Prasomsri, J. (2015). “Cyclic pore water pressure generation and stiffness degradation in compacted clays.” *Journal of Geotechnical and Geoenvironmental Engineering*, 142(1), 04015060.

Takada, N. (1993). “Mikasa’s direct shear apparatus, test procedures and results.” *Geotechnical Testing Journal*, 16(3), 314–322.

Tan, K. and Vucetic, M. (1989). “Behavior of medium and low plasticity clays under cyclic simple shear conditions.” *Proceedings of the 4th International Conference on Soil Dynamics and Earthquake Engineering. Mexico City:[sn]*, 131–142.

Thian, S. and Lee, C. (2017). “Cyclic stress-controlled tests on offshore clay.” *Journal of Rock*

622 *Mechanics and Geotechnical Engineering*, 9(2), 376–381.

623 Tsubakihara, Y., Kishida, H., and Nishiyama, T. (1993). “Friction between cohesive soils and steel.”

624 *Soils and Foundations*, 33(2), 145–156.

625 Uesugi, M. and Kishida, H. (1986). “Frictional resistance at yield between dry sand and mild steel.”

626 *Soils and foundations*, 26(4), 139–149.

627 Vucetic, M. and Dobry, R. (1988). “Degradation of marine clays under cyclic loading.” *Journal of*

628 *Geotechnical Engineering*, 114(2), 133–149.

629 Vucetic, M. and Lacasse, S. (1984). “Closure to “specimen size effect in simple shear test” by m.

630 vucetic and s. lacasse (december, 1982).” *Journal of Geotechnical Engineering*, 110(3), 447–453.

631 Wichtmann, T., Andersen, K., Sjursen, M., and Berre, T. (2013). “Cyclic tests on high-quality

632 undisturbed block samples of soft marine norwegian clay.” *Canadian Geotechnical Journal*,

633 50(4), 400–412.

634 Xiong, Y.-l., Liu, G.-b., Zheng, R.-y., and Bao, X.-h. (2018). “Study on dynamic undrained

635 mechanical behavior of saturated soft clay considering temperature effect.” *Soil Dynamics and*

636 *Earthquake Engineering*, 115, 673–684.

637 Yasuhara, K., Yamanouchi, T., and HIRAO, K. (1982). “Cyclic strength and deformation of normally

638 consolidated clay.” *Soils and Foundations*, 22(3), 77–91.

639 Yavari, N., Tang, A. M., Pereira, J.-M., and Hassen, G. (2016). “Effect of temperature on the

640 shear strength of soils and the soil–structure interface.” *Canadian Geotechnical Journal*, 53(7),

641 1186–1194.

642 Yazdani, S., Helwany, S., and Olgun, G. (2019). “Influence of temperature on soil–pile interface

643 shear strength.” *Geomechanics for Energy and the Environment*, 18, 69–78.

644 Zhou, J. and Gong, X. (2001). “Strain degradation of saturated clay under cyclic loading.” *Canadian*

645 *Geotechnical Journal*, 38(1), 208–212.

646

List of Tables

647 1 Kaolin clay physical and thermal properties. 29

648 2 Monotonic experimental program for a $\sigma'_{n0} = 300$ kPa and T= 22 ° C 30

649 3 Cyclic experimental program for a $\sigma'_{n0} = 300$ kPa. 31

TABLE 1. Kaolin clay physical and thermal properties.

Liquid limit, LL (%)	57%
Plastic limit, PL (%)	33%
Plasticity index, PI (%)	24%
Particle specific gravity, ρ_s (Mg/cm^3)	2.60
Thermal conductivity, λ (W/mK)	1.5
Heat capacity, C (J/m^3K)	3.3
Hydraulic conductivity, k (m/s)	1×10^{-8}

TABLE 2. Monotonic experimental program for a $\sigma'_{n0} = 300$ kPa and T= 22 ° C .

N^o	S_u^{Ds} (kPa)	w_i (%)	w_f (%)	\dot{P}_d (%/min)	e_0	Tt
1	56.4	62.3	37.2	0.01	0.835	clay-clay
2	56.4	63.3	43.2	0.02	0.828	clay-clay
3	63.1	59.6	36.0	0.01	0.844	clay-structure
4	63.2	60.5	36.2	0.02	0.836	clay-structure

w_i (%): initial water content at the beginning of consolidation, w_f (%): final water content at the end of shearing, e_0 (-): void ratio before shearing, Tt: test type.

TABLE 3. Cyclic experimental program for a $\sigma'_{n0} = 300$ kPa.

N^o	τ_a (kPa)	τ_{cy} (kPa)	S_u^{Ds} (kPa)	τ_a/S_u^{Ds} (-)	τ_{cy}/S_u^{Ds} (-)	T $^o(C)$	N_f (-)	w_i %	w_f %	e_0 (-)
6*	23	27	56.4	0.41	0.47	22 o	370	63.0	36.6	
7	26	36	63.1	0.41	0.57	22 o	39	63.0	36.6	0.870
8	26	36	63.1	0.41	0.57	60 o	165	61.4	39.3	0.832
9	26	34	63.1	0.41	0.54	22 o	46	60.9	36.4	0.812
10	26	34	63.1	0.41	0.54	60 o	137	61.7	35.7	0.868
11	26	30	63.1	0.41	0.47	22 o	185	60.7	42.5	0.852
12	26	30	63.1	0.41	0.47	60 o	645	63.0	35.1	0.784
13	26	22	63.1	0.41	0.35	22 o	4138	63.0	35.1	0.855
14	26	22	63.1	0.41	0.35	60 o	> 10000	61.6	35.1	0.804
15	28	34	63.1	0.44	0.54	22 o	65	62.4	37.8	0.825
16	28	34	63.1	0.44	0.54	60 o	111	61.7	38.0	0.793
17	30	30	63.1	0.47	0.47	22 o	230	62.2	36.5	0.840
18	30	30	63.1	0.47	0.47	22 o	246	61.3	(-)	(-)
19	30	30	63.1	0.47	0.47	60 o	991	61.2	35.0	0.788
20	24	30	63.1	0.47	0.38	22 o	57	62.5	37.3	0.833
21	24	30	63.1	0.47	0.38	60 o	355	61.4	35.6	0.806
22	30	22	63.1	0.47	0.35	22 o	> 1000	60.6	37.3	0.834
23	30	22	63.1	0.47	0.35	60 o	> 1000	61.3	40.4	0.794

*: clay-clay test. w_i (%): initial water content at the beginning of consolidation, w_f (%): final water content at the end of shearing. N_f (-): Number of cycle to failure, e_0 (-): void ratio before shearing.

650

List of Figures

651	1	Stress-strain behavior of soils under cyclic loading.	34
652	2	Temperature-controlled interface direct shear device.	35
653	3	Surface roughness profiles; (a) Measured profiles (b) Surface profile 2.	36
654	4	Cyclic thermo-mechanical path.	37
655	5	Monotonic constant-volume equivalent-undrained (CVEU) clay-clay and clay-	
656		structure interface tests.	38
657	6	Behavior of clay-structure interface under cyclic loading.	39
658	7	Clay-clay vs. clay-structure interface cyclic response.	40
659	8	(a) Thermal consolidation of clay-structure interface with a heating from 22 to 60	
660		°C; (b) Thermal vertical strain of clay-structure interface from 22 to 60 °C.	41
661	9	Effect of cyclic shear stress variation at different temperatures for $\tau_a/S_u^{Ds} = 0.41$	
662		and $\tau_{cy}/S_u^{Ds} = 0.35$ to 0.47 for clay-structure interface tests. (a) Shear strain vs.	
663		number of cycles; (b) permanent shear strain vs. number of cycles; (c) equivalent	
664		pore pressure vs. number of cycles; (d) degradation index vs. number of cycles. . .	42
665	10	Effect of cyclic shear stress variation at different temperatures for $\tau_a/S_u^{Ds} = 0.47$	
666		and $\tau_{cy}/S_u^{Ds} = 0.35$ and 0.47 for clay-structure interface tests. (a) Shear strain vs.	
667		number of cycles; (b) permanent shear strain vs. number of cycles; (c) equivalent	
668		pore pressure vs. number of cycles; (d) degradation index vs. number of cycles. . .	43
669	11	Effect of average shear stress variation at different temperatures for $\tau_{cy}/S_u^{Ds} = 0.54$	
670		and $\tau_a/S_u^{Ds} = 0.41$ and 0.44 for clay-structure interface tests. (a) Shear strain vs.	
671		number of cycles; (b) permanent shear strain vs. number of cycles; (c) equivalent	
672		pore pressure vs. number of cycles; (d) degradation index vs. number of cycles. . .	44
673	12	Effect of average shear stress variation at different temperatures for $\tau_{cy}/S_u^{Ds} = 0.47$	
674		and $\tau_a/S_u^{Ds} = 0.38$ to 0.47 for clay-structure interface tests. (a) Shear strain vs.	
675		number of cycles; (b) permanent shear strain vs. number of cycles; (c) equivalent	
676		pore pressure vs. number of cycles; (d) degradation index vs. number of cycles. . .	45

677	13	Monotonic and cyclic strain-softening comparison in (a) clay-clay test and (b)	
678		clay-structure interface test.	46
679	14	Cyclic loops comparison for clay-clay and clay-structure tests at 22 °C (a) N=1 (b)	
680		N=10 (c) N=100. $P_d^*(\%)$ = shear strain from the beginning of cycle N.	47
681	15	Cyclic loops at different temperatures $P_d^*(\%)$ = relative lateral displacement from	
682		the beginning of cycle N.	48
683	16	Evolution of degradation parameter (t), with cyclic stress ratio variation at different	
684		temperatures (22 and 60 °C).	49
685	17	(a) τ_{cy}/S_u^{Ds} vs number of cycles curve for different relative lateral displacements;	
686		(b) $u^*/\sigma'_{n,i}$ vs number of cycles curve for certain values of normalized equivalent	
687		pore pressure.	50

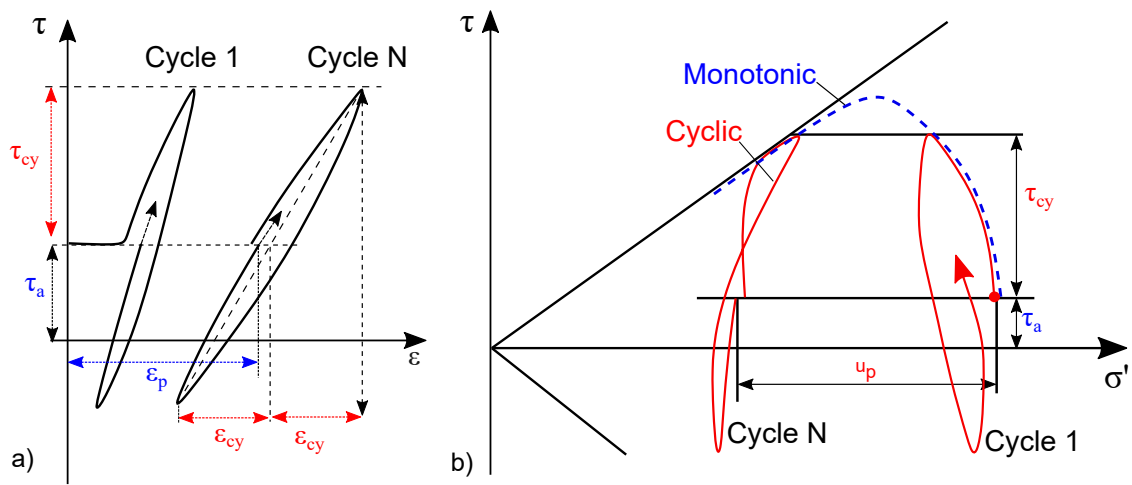


Fig. 1. Stress-strain behavior of soils under cyclic loading.

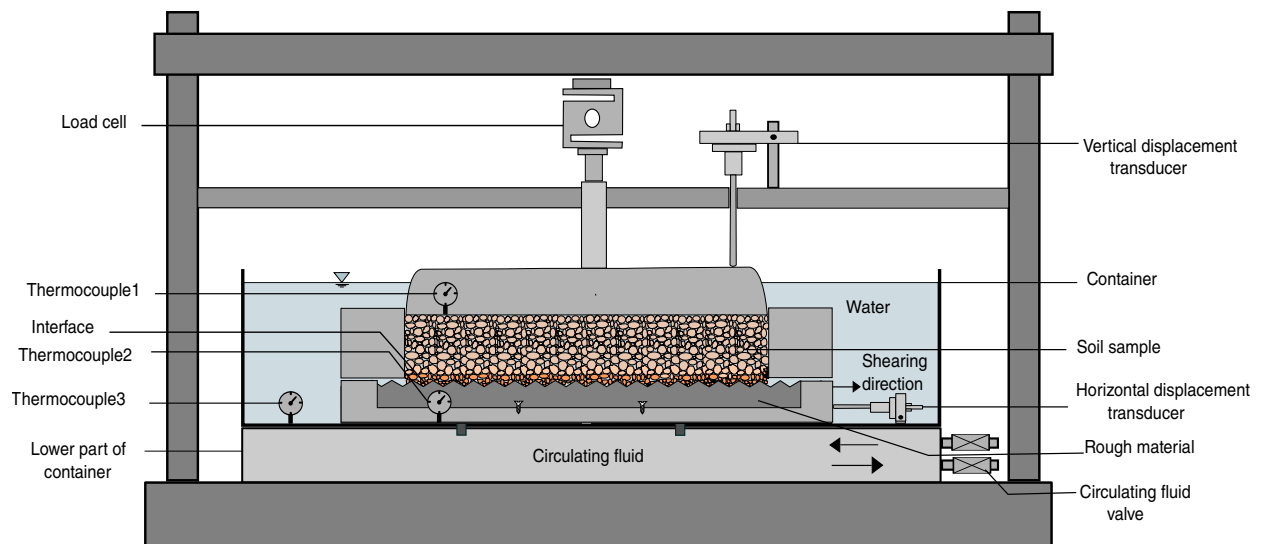


Fig. 2. Temperature-controlled interface direct shear device.

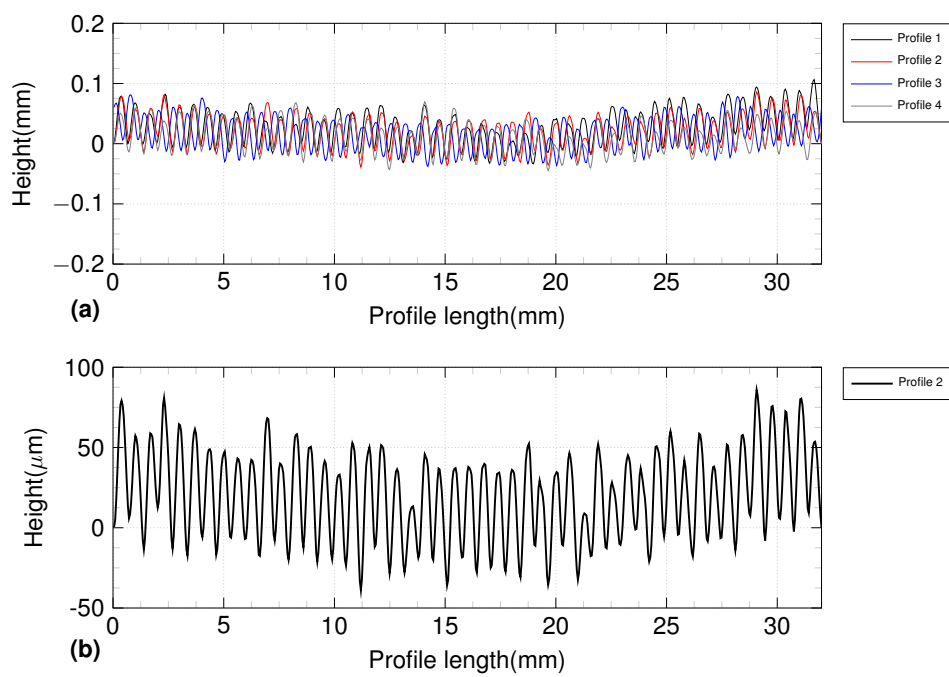


Fig. 3. Surface roughness profiles; (a) Measured profiles (b) Surface profile 2.

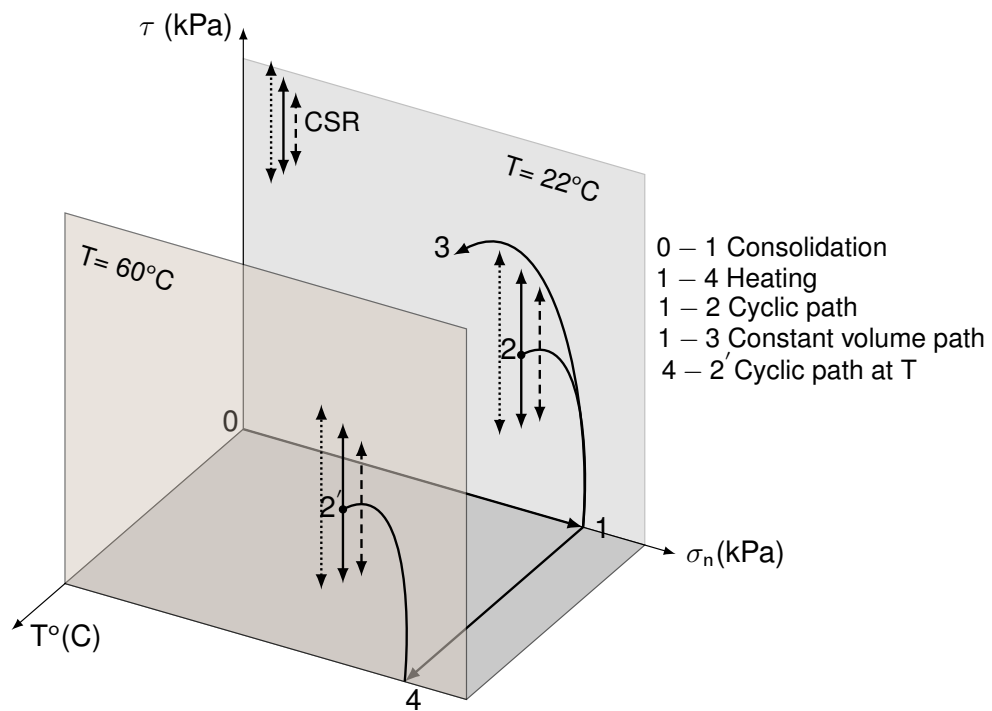


Fig. 4. Cyclic thermo-mechanical path.

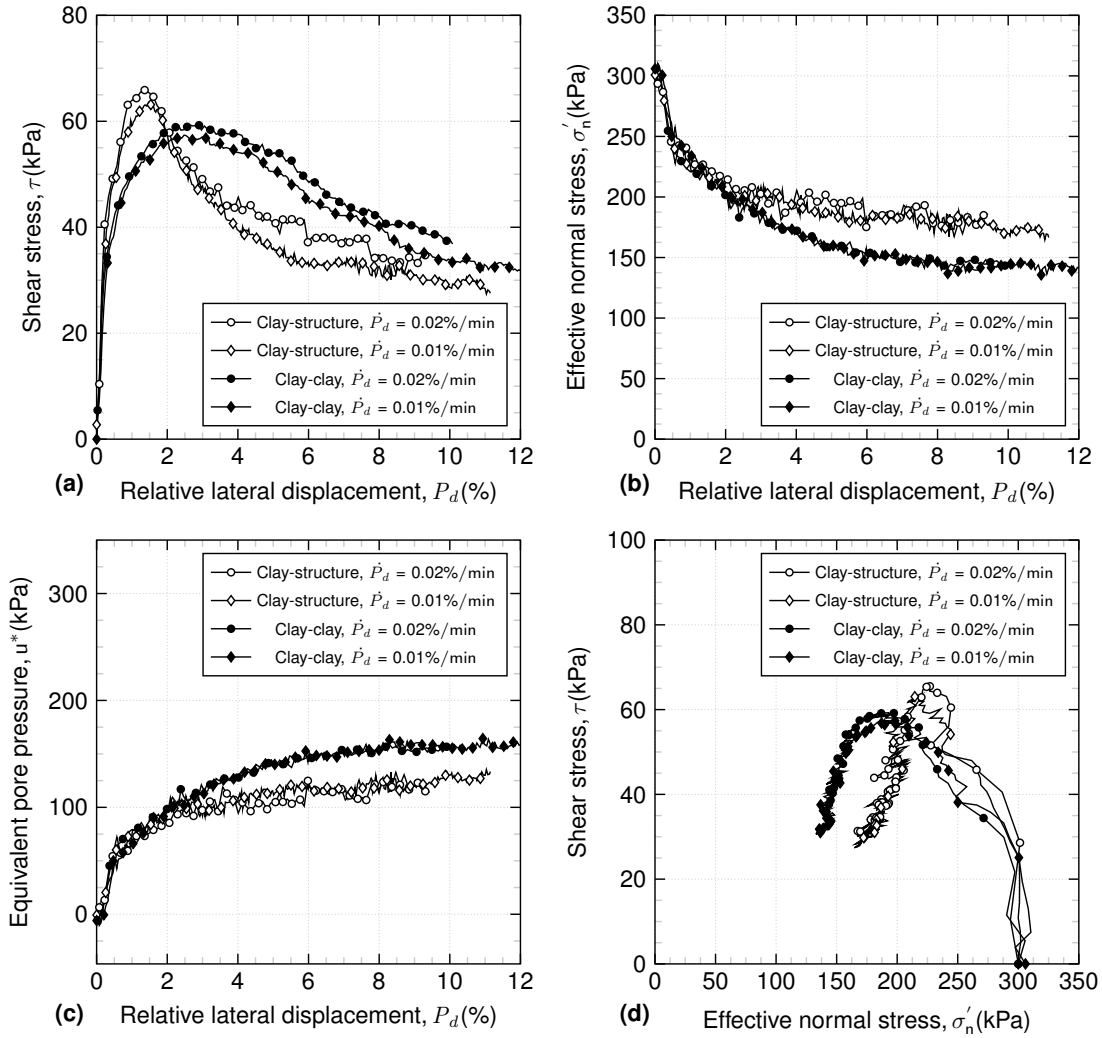


Fig. 5. Monotonic constant-volume equivalent-undrained (CVEU) clay-clay and clay-structure interface tests.

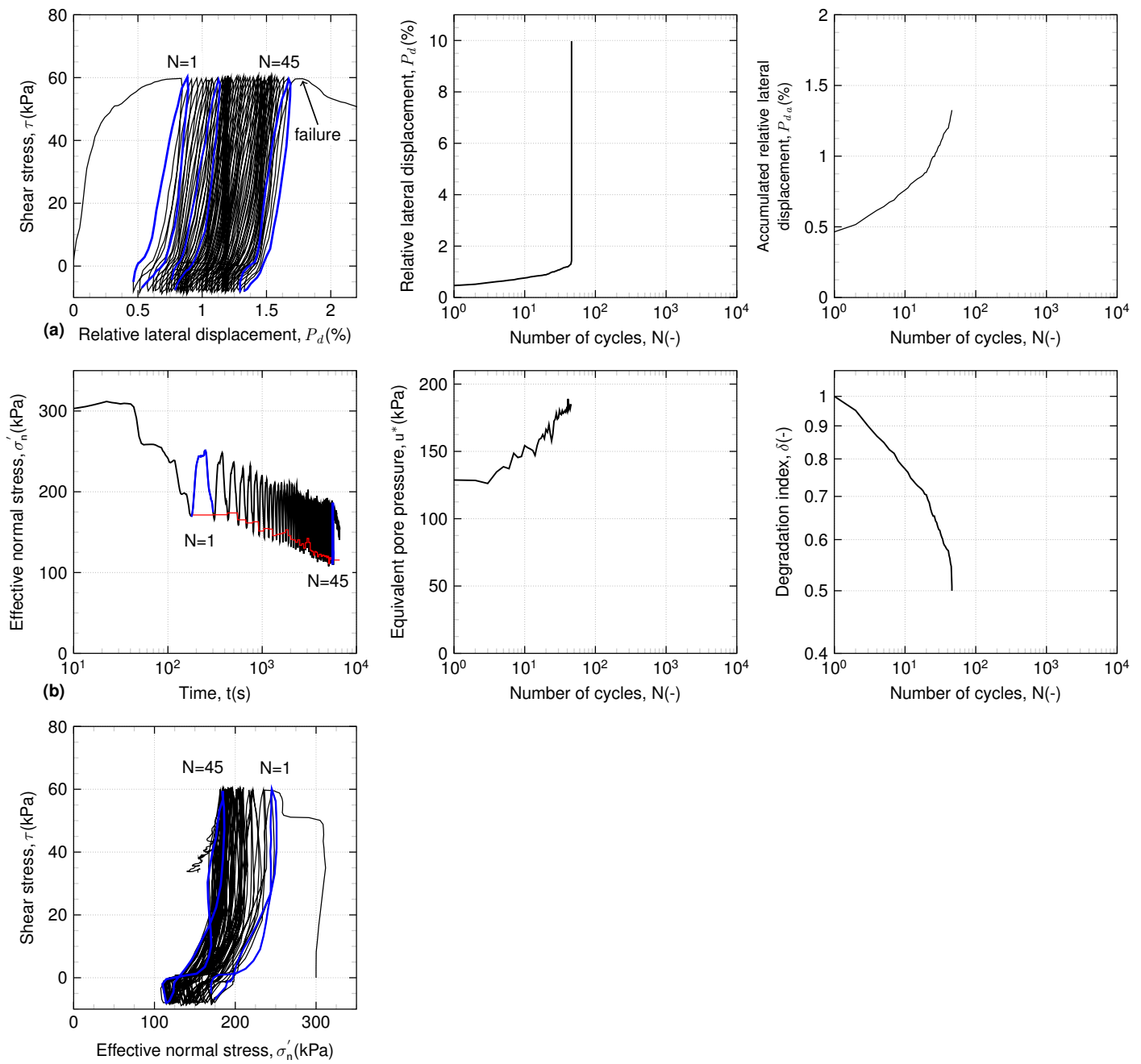


Fig. 6. Behavior of clay-structure interface under cyclic loading.

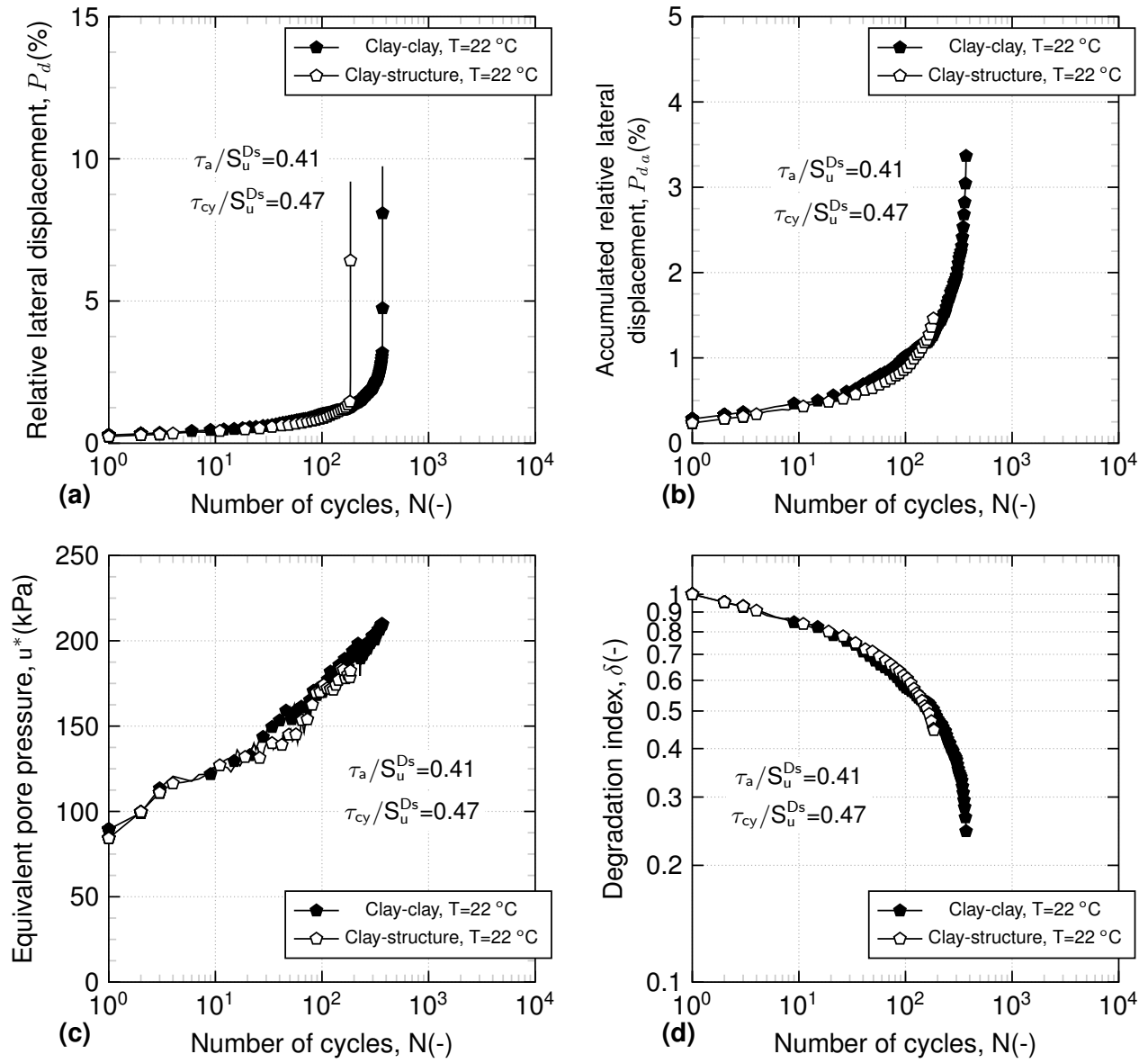


Fig. 7. Clay-clay vs. clay-structure interface cyclic response.

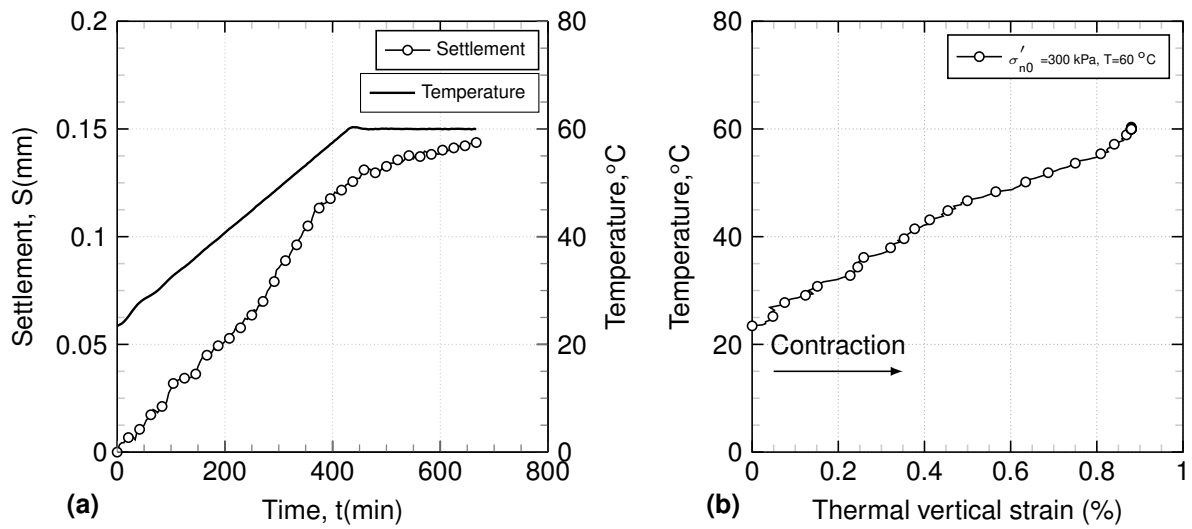


Fig. 8. (a) Thermal consolidation of clay-structure interface with a heating from 22 to 60 $^{\circ}\text{C}$; (b) Thermal vertical strain of clay-structure interface from 22 to 60 $^{\circ}\text{C}$.

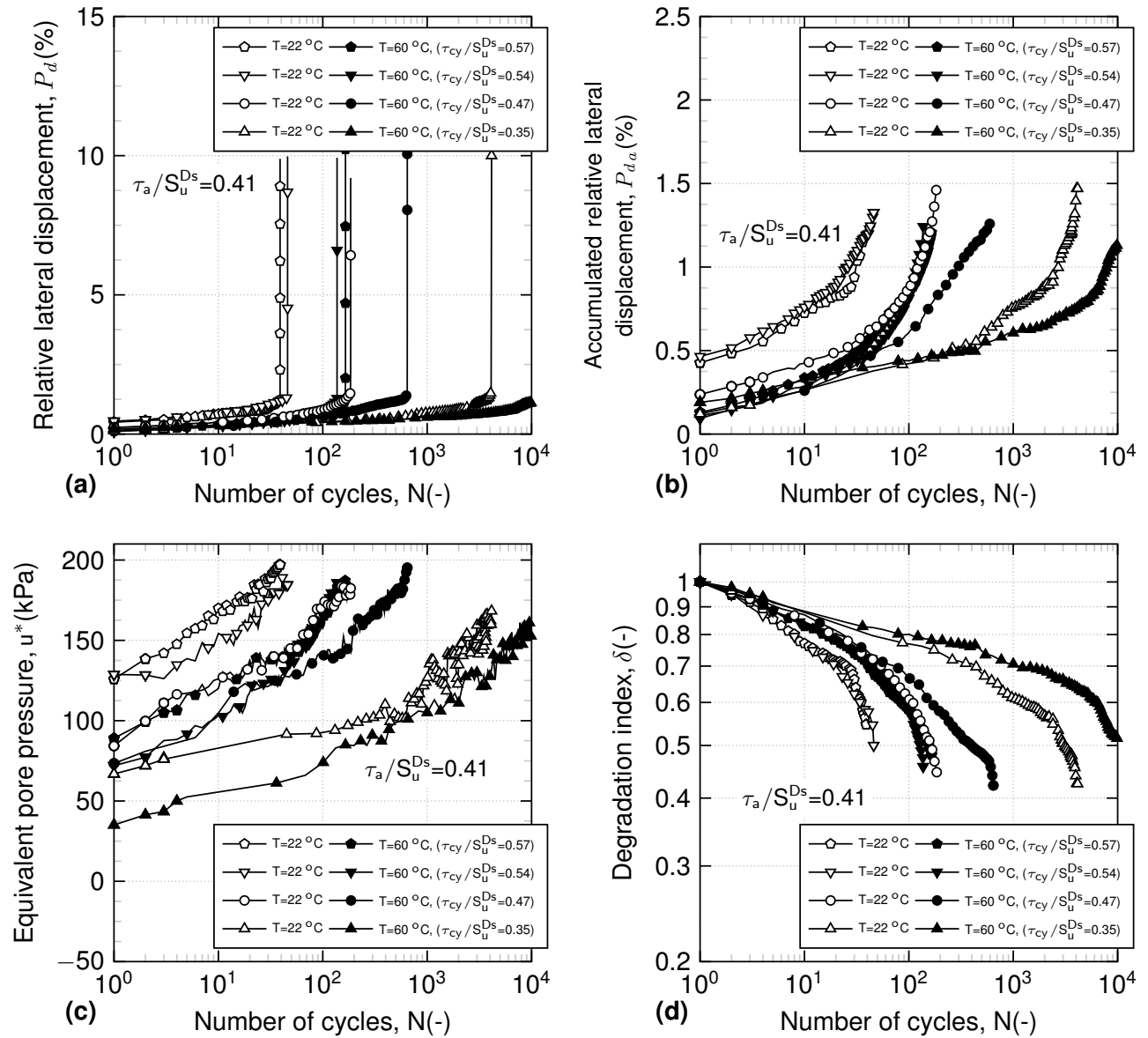


Fig. 9. Effect of cyclic shear stress variation at different temperatures for $\tau_a/S_u^{Ds} = 0.41$ and $\tau_{cy}/S_u^{Ds} = 0.35$ to 0.47 for clay-structure interface tests. (a) Shear strain vs. number of cycles; (b) permanent shear strain vs. number of cycles; (c) equivalent pore pressure vs. number of cycles; (d) degradation index vs. number of cycles.

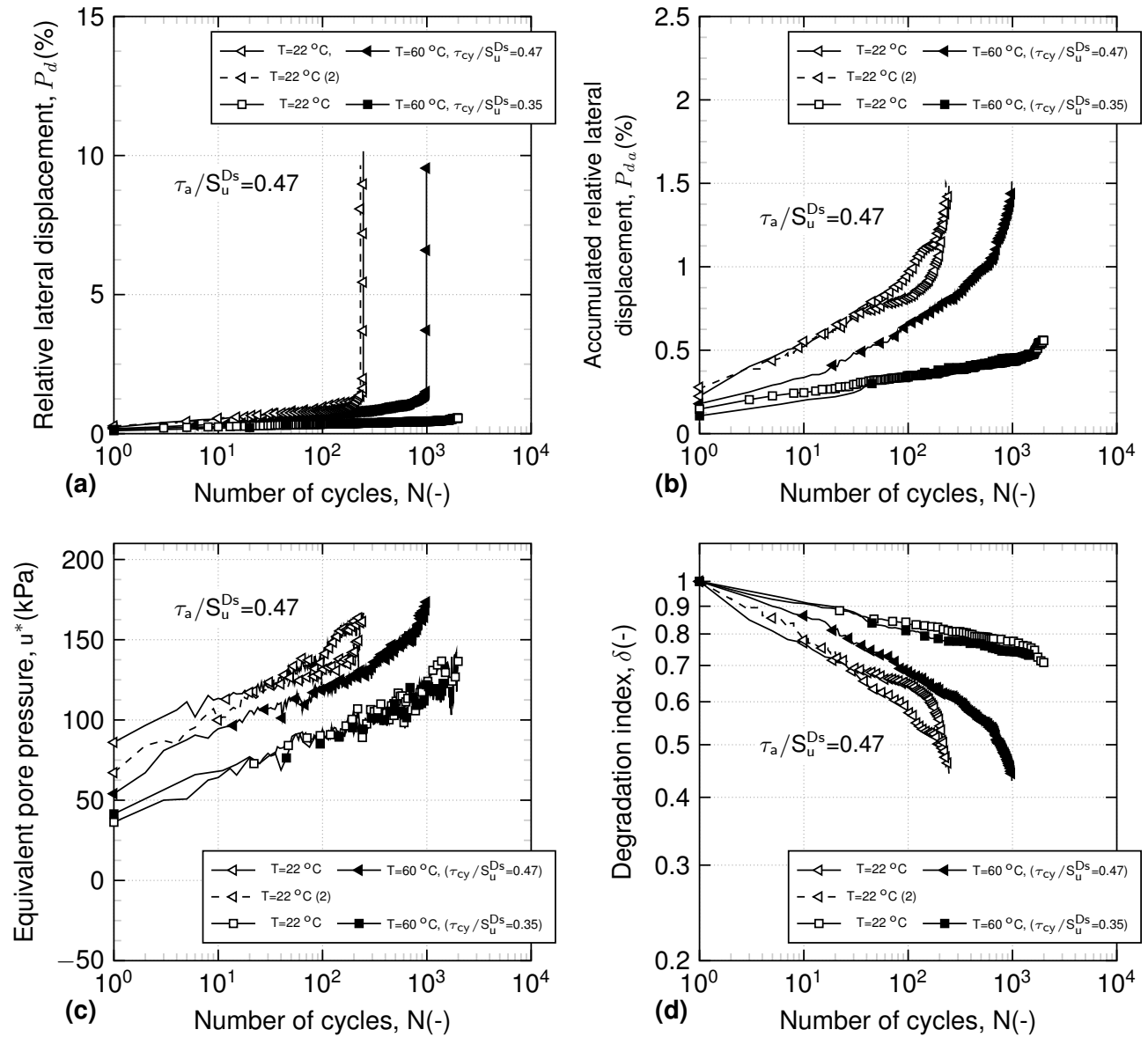


Fig. 10. Effect of cyclic shear stress variation at different temperatures for $\tau_a/S_u^{Ds} = 0.47$ and $\tau_{cy}/S_u^{Ds} = 0.35$ and 0.47 for clay-structure interface tests. (a) Shear strain vs. number of cycles; (b) permanent shear strain vs. number of cycles; (c) equivalent pore pressure vs. number of cycles; (d) degradation index vs. number of cycles.

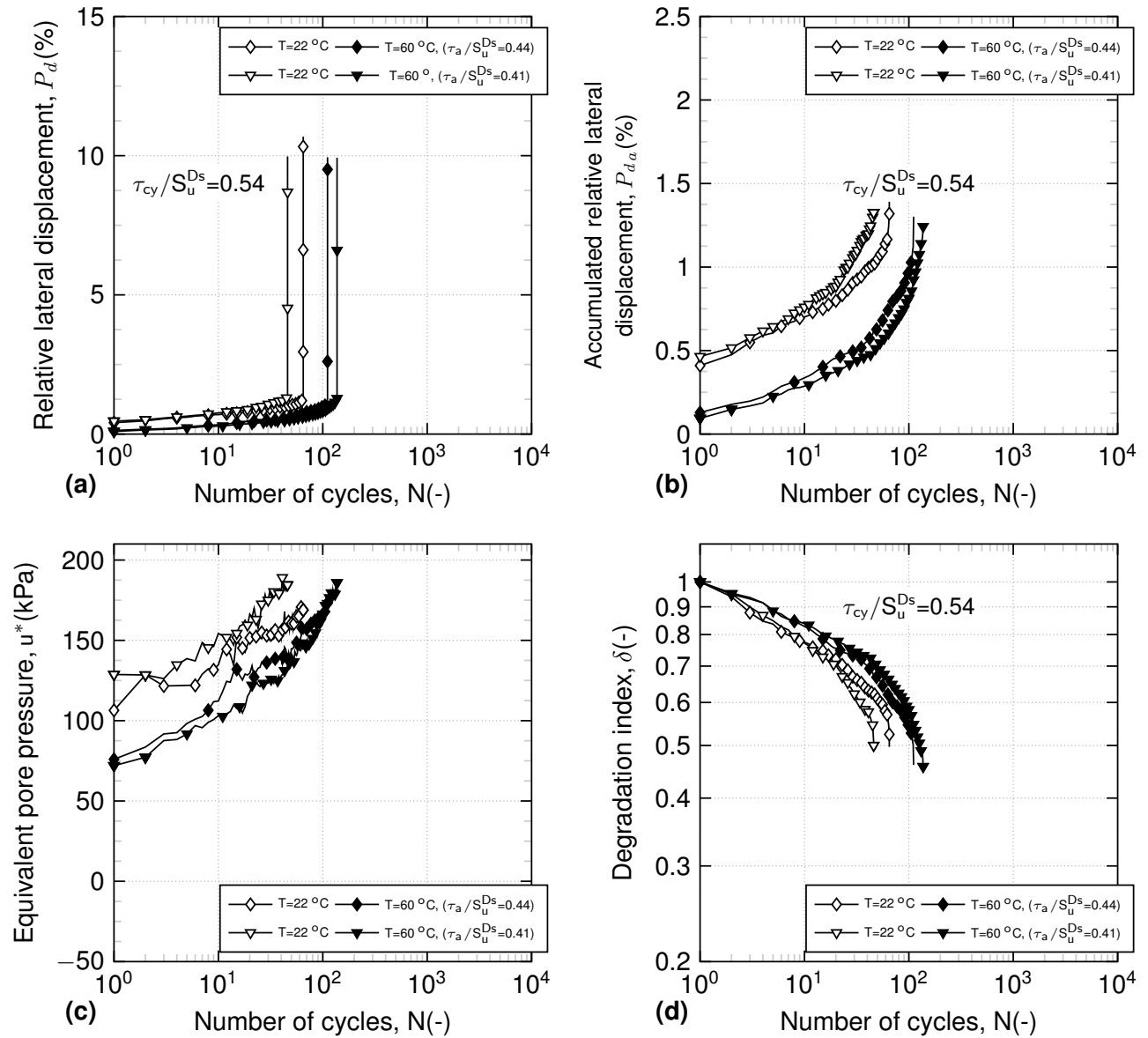


Fig. 11. Effect of average shear stress variation at different temperatures for $\tau_{cy}/S_u^{Ds} = 0.54$ and $\tau_a/S_u^{Ds} = 0.41$ and 0.44 for clay-structure interface tests. (a) Shear strain vs. number of cycles; (b) permanent shear strain vs. number of cycles; (c) equivalent pore pressure vs. number of cycles; (d) degradation index vs. number of cycles.

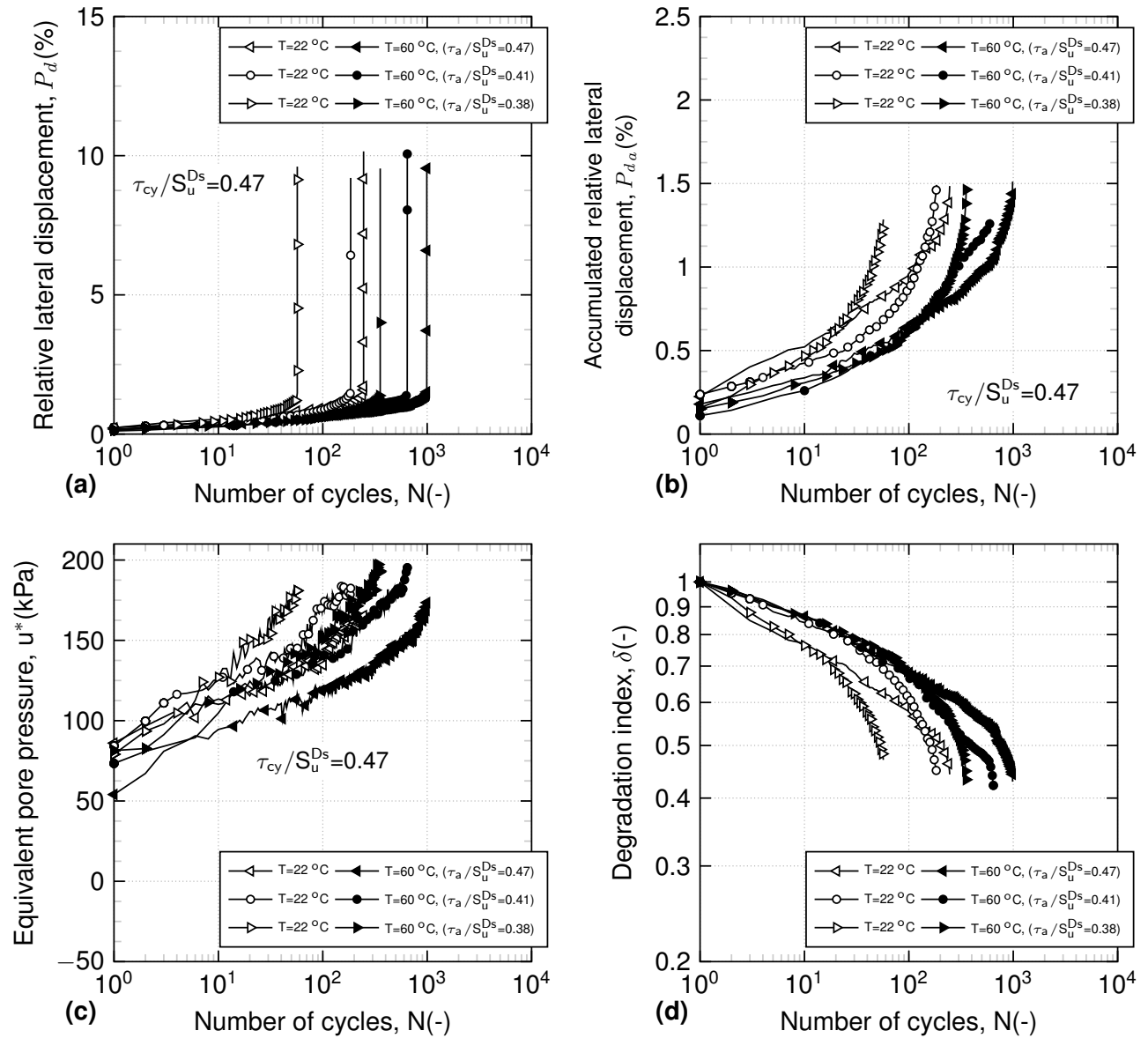


Fig. 12. Effect of average shear stress variation at different temperatures for $\tau_{cy}/S_u^{Ds} = 0.47$ and $\tau_a/S_u^{Ds} = 0.38$ to 0.47 for clay-structure interface tests. (a) Shear strain vs. number of cycles; (b) permanent shear strain vs. number of cycles; (c) equivalent pore pressure vs. number of cycles; (d) degradation index vs. number of cycles.

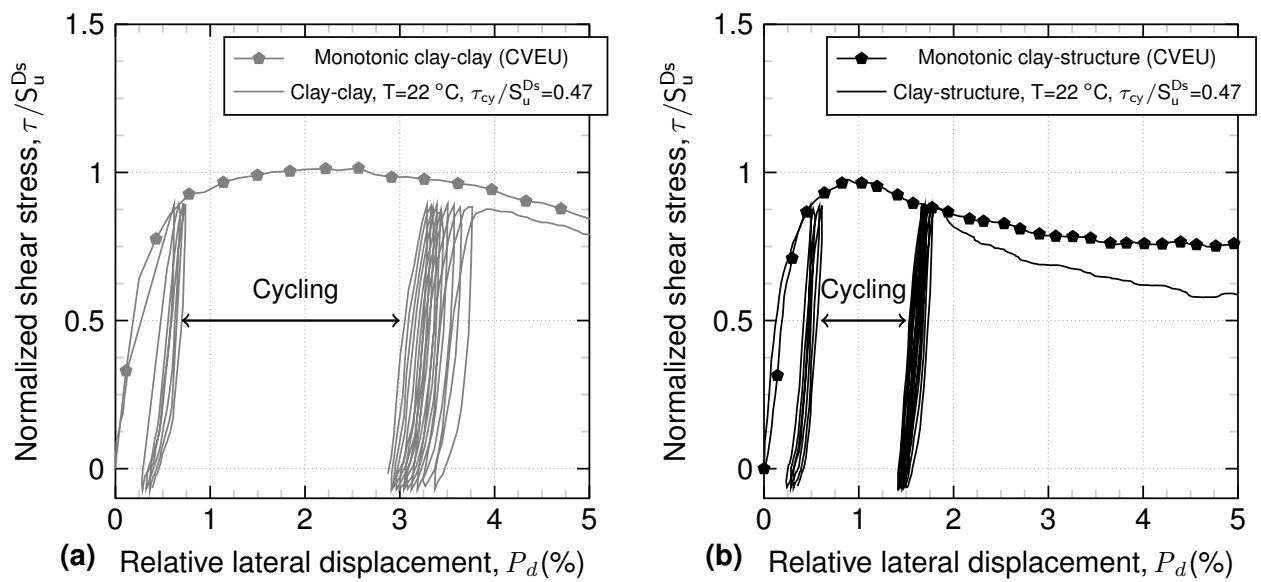


Fig. 13. Monotonic and cyclic strain-softening comparison in (a) clay-clay test and (b) clay-structure interface test.

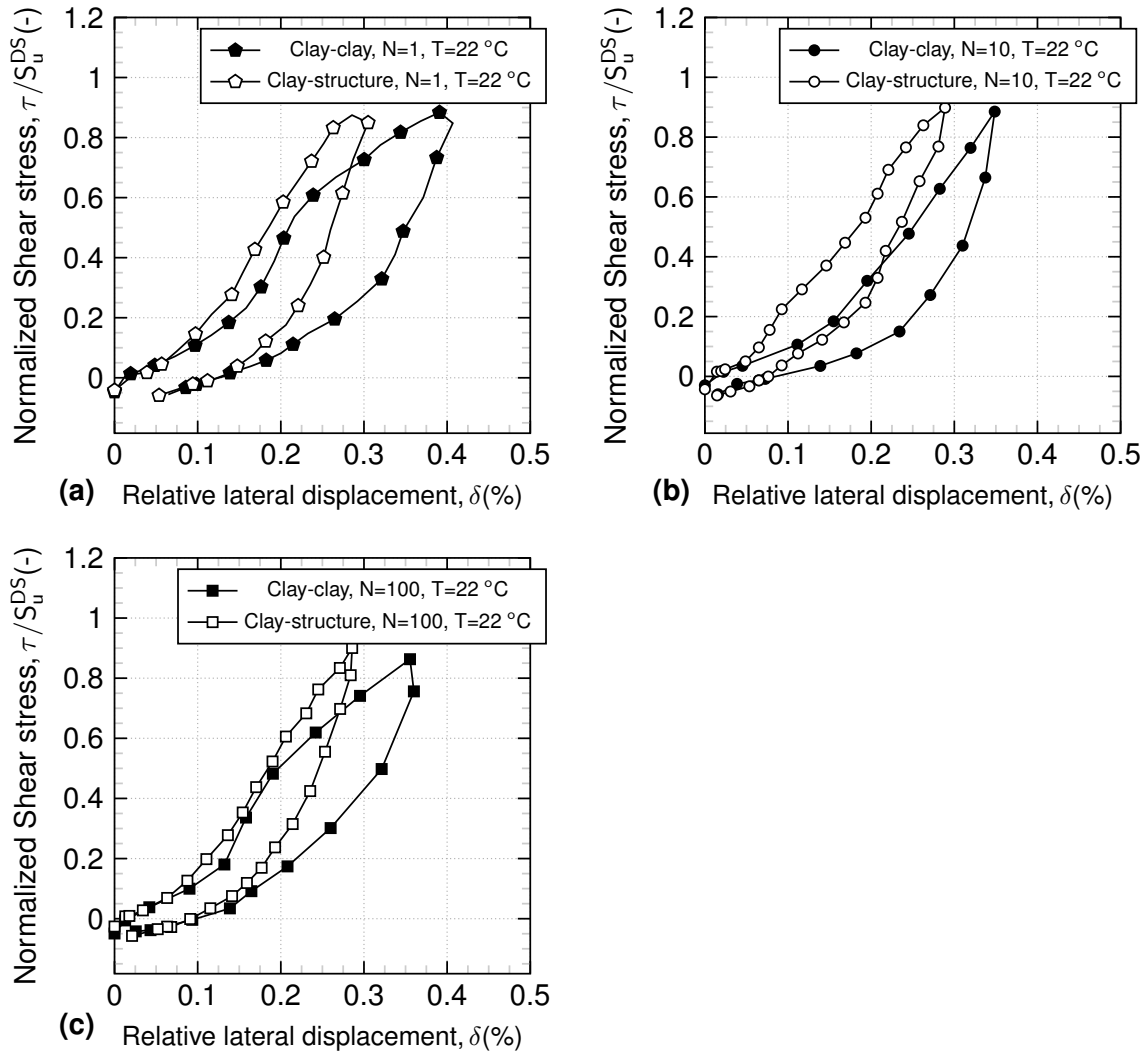


Fig. 14. Cyclic loops comparison for clay-clay and clay-structure tests at 22 °C (a) N=1 (b) N=10 (c) N=100. P_d^* (%) = shear strain from the beginning of cycle N.

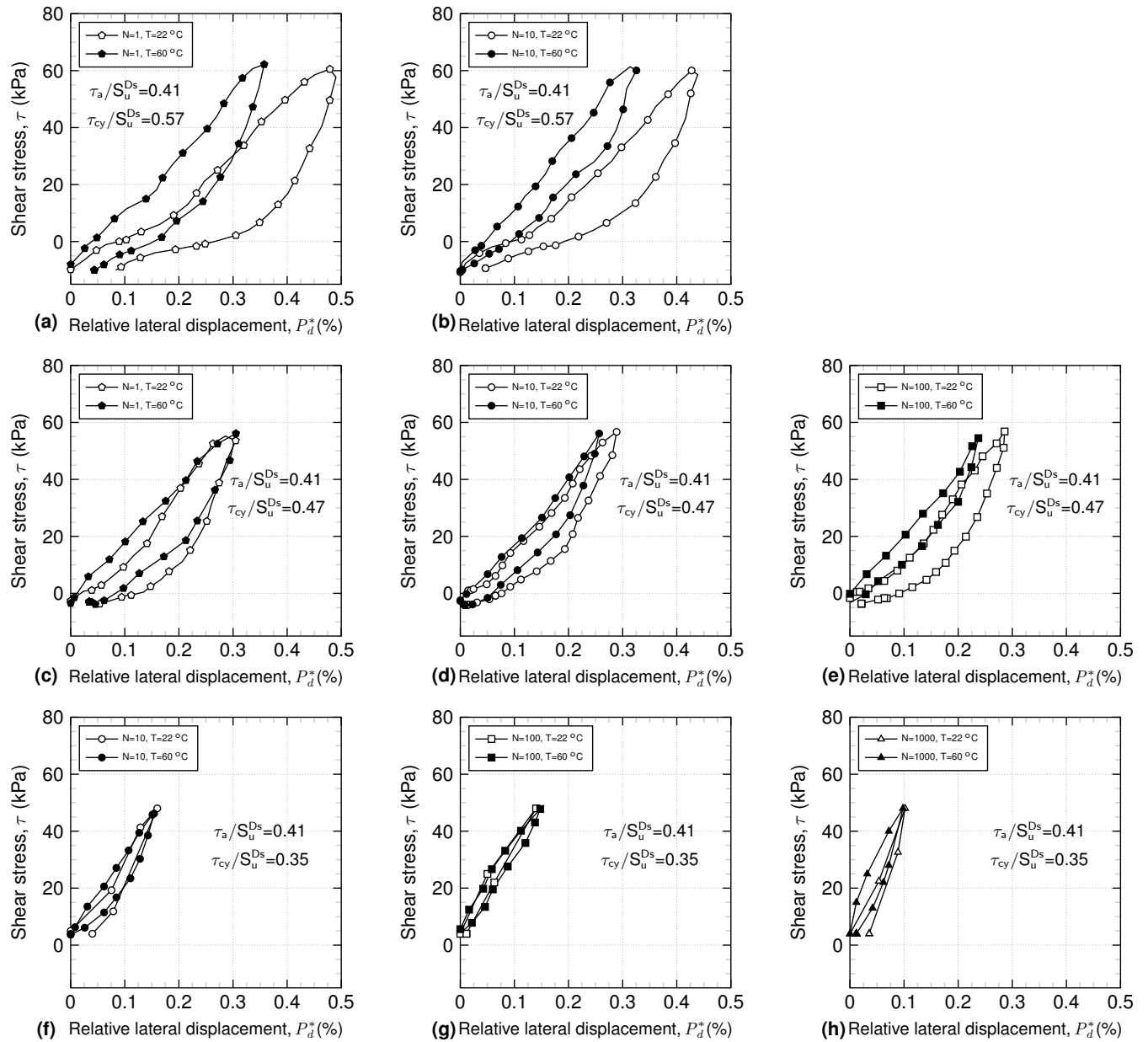


Fig. 15. Cyclic loops at different temperatures $P_d^*(\%)$ = relative lateral displacement from the beginning of cycle N.

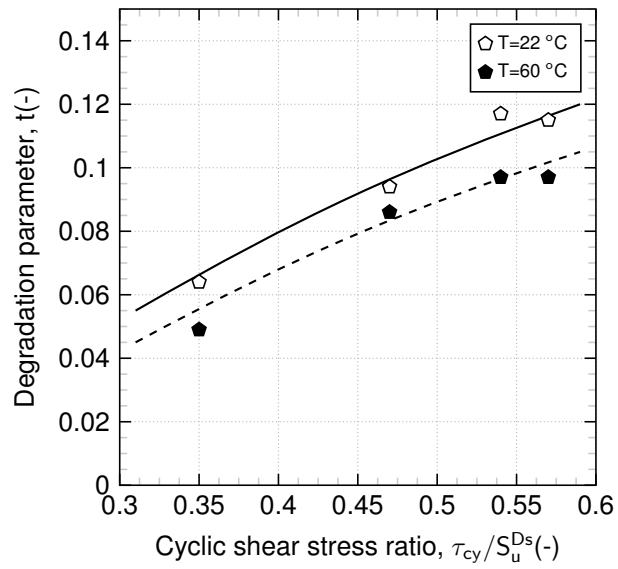


Fig. 16. Evolution of degradation parameter (t), with cyclic stress ratio variation at different temperatures (22 and 60 °C).

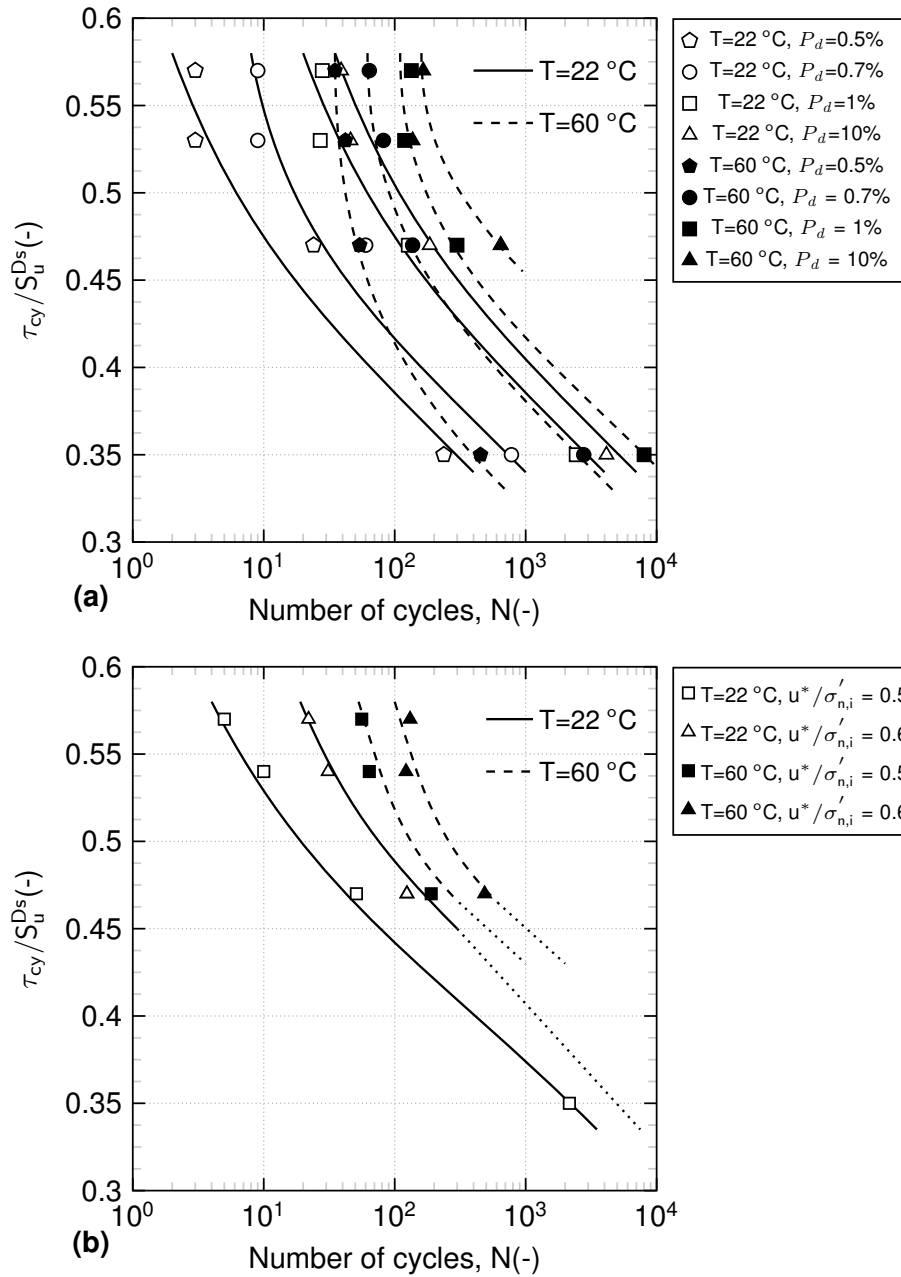


Fig. 17. (a) τ_{cy}/S_u^{Ds} vs number of cycles curve for different relative lateral displacements; (b) $u^*/\sigma'_{n,i}$ vs number of cycles curve for certain values of normalized equivalent pore pressure.